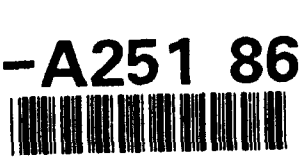

(1)

FINAL TECHNICAL REPORT
Item Number Supplies/Services: 0002

For: GUIDED-WAVE TeO_2 ACOUSTO-OPTIC DEVICES.

Contract Number: DAAL02-90-C-0053

Issued by: ISA/LABCOM Directorate of Contracting, Code W71BFJ
2800 Powder Mill Road
Adelphi, Maryland 20783-1197

Attn: Luis Mudd, SLCIS-C-C

Covering: June 15,1990 to Jan. 5, 1991

Deliver to: Harry Diamond Laboratories
Attn: Mrs. Lora J. Harrison
2800 Powder Mill Rd.
Adelphi, MD. 20783-1197

Prepared by: OPTECH LABORATORY, Code OLBH8
22048 Sherman Way #113
Canoga Park, CA. 91303

Preparation Date: Jan. 12, 1991

--- Unclassified ---

TABLE OF CONTENTS

Accesion For	
NTIS CRA&I	☒
DTIC TAB	☐
Unannounced	☐
Justification	
By	
Distribution /	
Availability Codes	
Dist	Avail and / or Special
A-1	

Statement A per telecon Lora Harrison
Harry Diamond Laboratories
ATTN: SLCHD-SP-OP
Adelphi, MD 20783-1197
NWW 6/18/92

1.0. INTRODUCTION:

In this research program, Guided-Wave TeO_2 Acousto-Optic Devices, the properties of surface acoustic waves on tellurium dioxide single crystal surfaces has been studied for its potential applications as acousto-optic signal processing devices. Personal computer based numerical method has been utilized for searching of useful surface acoustic waves and for theoretical investigation of the properties of surface acoustic waves on tellurium dioxide crystal substrate. Particular emphasis is on the finding and exploration of slow surface acoustic waves for long delay time signal processing applications.

The investigation also includes study of surface acoustic wave interaction with laser beams after total internal reflection beneath the surface of the crystal substrate. The usefulness of such interaction for optical signal processing applications is also investigated in comparison to similar devices using the bulk slow shear waves in TeO_2.

Based on theoretical study results, several TeO_2 substrate have been prepared. Surface acoustic waves have been launched onto these sample substrate using edge coupled shear wave transducers. Experiments has been conducted for surface acoustic wave interaction with laser beams. Use of the acousto-optic probe, the surface acoustic wave velocity and field distribution have been obtained and compared to theoretical data.

A 70 micro-second bulk slow shear wave acousto-optic beam deflector has been fabricated for comparison. Advantages of the surface acoustic wave beam deflector over bulk wave deflectors are considered. Potential applications as well as areas for further developments are recommended for a phase II development program.

1.1. BACKGROUND:

Acousto-optical signal processing technology is very important for applications such as radar threat warning receivers, communication signal correlators, synthetic aperture radar signal processing, and geolocation devices. Key parameters for acousto-optical devices are signal processing time, bandwidth, efficiency-bandwidth product, spurious responses (e.g. third order intermodulation products), and optical insertion loss. Long device signal processing time is one of the parameters difficult to achieve since requiring long device length and slow acoustic velocity. Physical length of signal processing device is usually limited by the availability of large crystals, the attenuation of acoustic wave, and the overall system dimension necessary to accommodate a large optical aperture. Yet in many applications such as the highly successful acousto-optical correlators, long signal processing is required for long signal search window or for the time integration of long signal bit streams.

A practical approach to achieve long signal processing time in acousto-optical devices is to use slow acoustic modes such as the slow shear waves in TeO_2, or in $HgCl_2$

crystals. The slow acoustic velocity also contributes to exceptional large acousto-optical figure of merits which is inversely proportional to the cubic of acoustic velocity. However, these local velocity minimum directions always come with magnified acoustic beam divergence angle and thus large diffraction loss due to poynting vector walk-offs on off-axis wave components in anisotropic medium. Such acoustic diffraction loss are significant in devices with long delay time unless the acoustic transducers are made very large to minimize the off-axis wave components. For instance, the anisotropic diffraction factor for the <110> slow shear wave of TeO_2 is about 50 in the (001) plane, and is about 35 in the (-110) plane. To control the diffraction loss, the transducer height is usually made about 7 times larger than for the case of isotropic modes. As a result, proportionally larger drive power is required.

Use of acoustic surface wave reduces the diffraction phenomena to 2-dimensional. The acoustic diffraction loss is thus significantly reduced. The effective acoustic beam height is only a few acoustic wavelengths. For instance, a 50 Mhz on-axis slow shear TeO_2 bulk acousto-optic deflector with 70 microsecond delay time will require a transducer height of 6mm. By first order estimation, use of acoustic surface wave may reduce the effective transducer height to 17 micron, corresponding to an improvement of 360 in efficiency. In addition, current applications of slow shear wave TeO_2 devices are limited to bandwidth of less than 50 MHz due to loss considerations. Reduction in acoustic diffraction loss may expand the useful bandwidth of slow wave Bragg cells.

The significance of a new acousto-optic Bragg cell using slow surface acoustic waves will be greater useful bandwidth and time-bandwidth product, potentially longer signal processing time, and extremely low drive power requirement. The drive power may be in the order of milli-watts making miniaturization of signal processing systems possible.

The study of surface acousto-optic Bragg cell is a very interesting and really challenging subject involving many disciplines. Technical issues include (1) wideband high efficiency SAW generation on TeO_2, (2) search for appropriate slow SAW modes with non-oscillating field into the substrate, (3) calculating the surface acousto-optic interaction strength for the promising SAW modes, (4) improving the acousto-optic interaction length by waveguiding means, (5) use of phased array techniques for abnormal Bragg interaction devices, and (6) finding the acoustic propagation properties such as anisotropic diffraction, propagation loss, etc. of the interested acoustic surface waves. Analytical work is critically important to finding proper crystal orientations for useful slow SAW and to develop simple and manufacturable devices.

1.2. PHASE I PROGRAM OBJECTIVES:

The objective of the overall program is to develop extremely efficient wideband large time-bandwidth product and low spurious response acousto-optic Bragg cells using surface acoustic waves on TeO_2 substrate.

The phase I program objective is to investigate the possibilities and the potential of advanced guidedwave acousto-optic Bragg cells based on surface acoustic waves in TeO_2 for improved long signal processing time spatial light modulators. Analytical modeling on surface acoustic waves, surface acousto-optic interaction, acoustic waveguide, and advanced phased array techniques, will be conducted when necessary. Experimental devices will be fabricated for verification of analytical findings. Surface acoustic wave data and surface acousto-optic interaction data will be collected from these samples and will be compared to bulk wave data. Based on results from these systematic investigation, devices having time-bandwidth product greater than 1000 will be designed. Possibility of incorporate two counter-propagating acoustic waves will be studied. Surface acoustic wave samples will be provided to the army for further evaluation.

The analytical and experimental results and design examples of phase I program will be used as guideline for the development of improved slow wave bulk and surface acousto-optic Bragg cells during the phase II program.

1.3. PHASE I SUMMARY:

During the phase I program, we have investigated the properties of surface acoustic waves on tellurium dioxide single crystal surfaces for its potential applications as acousto-optic signal processing devices. Personal computer based numerical method has been [1-3] utilized for searching of useful surface acoustic waves and for theoretical investigation of the properties of surface acoustic waves on tellurium dioxide crystal substrate.

A slow surface acoustic wave propagating along the <110> directions on (-110) cut substrate has been found with great potential for long delay time signal processing applications. This slow surface acoustic wave consists mostly of the slow shear wave acoustic component and is weakly guided along the surface. The velocity of this slow SAW is only slightly slower than the velocity of the slow shear wave. The slow SAW field penetrates deeply into the crystal for a half amplitude point of about 50 wavelengths as compared to one wavelength for typical surface acoustic waves. The relatively deep SAW field penetration is good for interaction with a focusing laser beam.

Based on theoretical study results, several TeO_2 substrate have been prepared. Surface acoustic waves have been launched onto these sample substrate using edge coupled shear wave transducers. Experiments has been conducted for surface acoustic wave interaction with laser beams. Use of the acousto-optic probe, the surface acoustic wave velocity and field distribution have been obtained and the accuracy of theoretical data has been verified.

In addition, surface acousto-optic interaction between the slow SAW and a free propagating focused laser beam reflecting from the underside of the crystal surface has been analyzed. Surface acousto-optic interaction design data has been generated. The

usefulness of such interaction for optical signal processing applications is found favorable in comparison with similar devices using bulk slow shear waves in TeO_2. A 70 micro-second bulk slow shear wave acousto-optic beam deflector has been fabricated for verifying the comparison.

Analytical study has been carried out for the case of counter propagating acousto-optic Bragg cells for correlator applications. Using the device design guidelines derived during this program, preliminary slow SAW counter propagating Bragg cell has been designed for signal processing applications and recommended for phase II developments.

2.0. TECHNICAL RESULTS:

2.1. THEORETICAL INVESTIGATION OF SAW ON TeO_2:

2.1.1. VALIDATING THE COMPUTER MODEL:

The acoustic waves in solids can be calculated by solving the wave equations subject to boundary value conditions at the solid-air interface. The wave solutions are assumed periodical with decaying amplitude into the substrate. The simultaneous equations due to the boundary conditions yields the characteristics equation which can be solved for wave velocities and decay constants. Substituting the wave parameters back to the equation yields the surface acoustic field components.

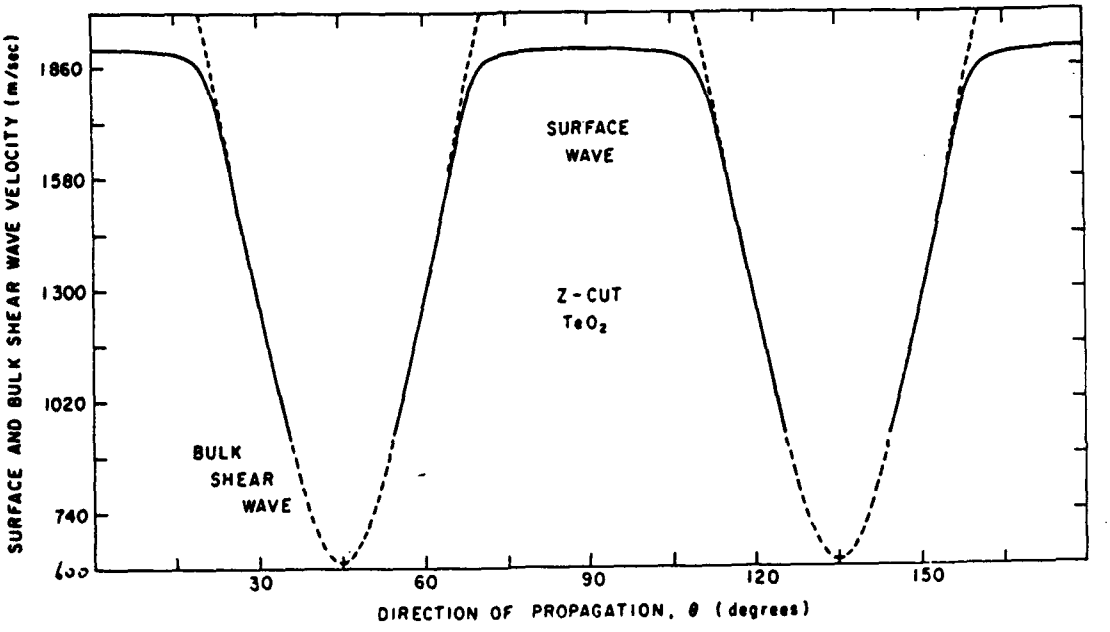

Figure 1, Surface Acoustic Wave Velocity Surface on (001) Cut TeO_2.

A PC based computer model was used to calculate the surface acoustic waves on various cuts of TeO_2. The model has been published by E.L. Adler, et al., on Ultrasonics International 85, Proceedings, 1985. The analytical process begins with calculation of surface acoustic waves on known orientations of tellurium dioxide and compare the results with data from open literature.[4-6] After that, the computer model was used to search for a slow surface acoustic wave and its physical properties.

The validity and accuracy of the computer model and material parameters is first tested on well known materials and acoustic waves. The calculated velocity surfaces of bulk waves in $LiNbO_3$, in TeO_2, in $PbMoO_4$, and in GaP, and the results are in excellent agreement with published data. Next, the surface acoustic wave velocity and field distribution on $LiNbO_3$ is calculated and is compared to published data[5] on "Microwave Acoustics Handbook, Vol.1A, Surface Wave Velocities," by Slobodnik Jr., et.al. also with excellent agreement. The last test is conducted on several cuts of TeO_2 on which surface acoustic wave data can be found on "Microwave Acoustics Handbook" also and is given by figure 1, figure 2, and figure 3, for the case of x-cut and z-cut plates. Again, excellent agreement is found between our computer model and published data.

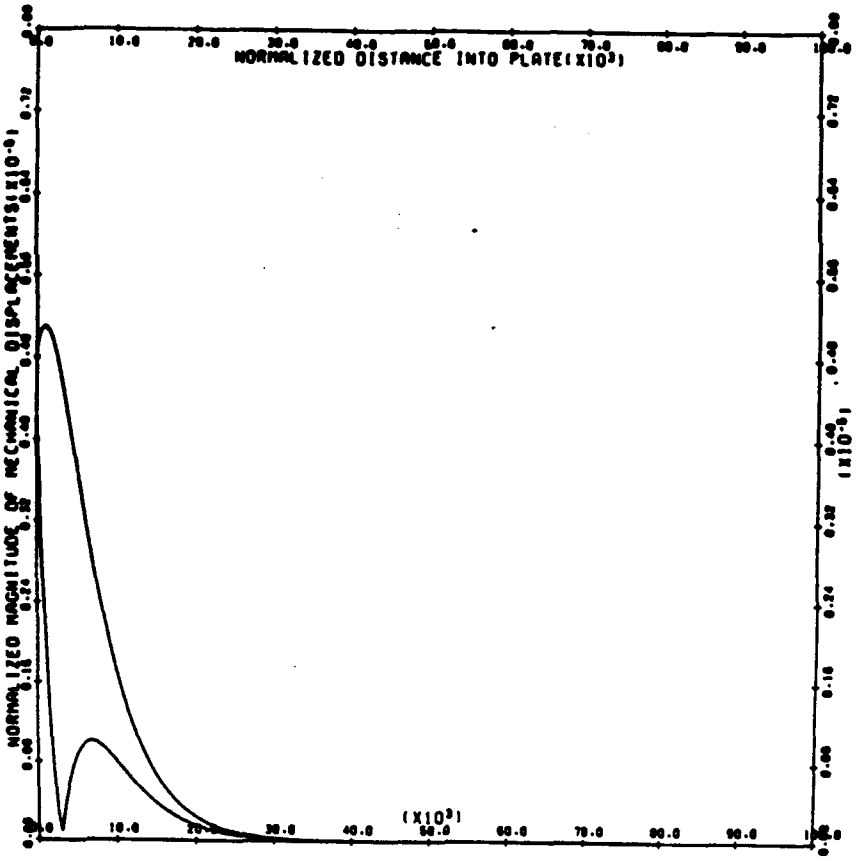

Figure 2, Field Components of Surface Acoustic Wave on (001) Cut TeO_2.

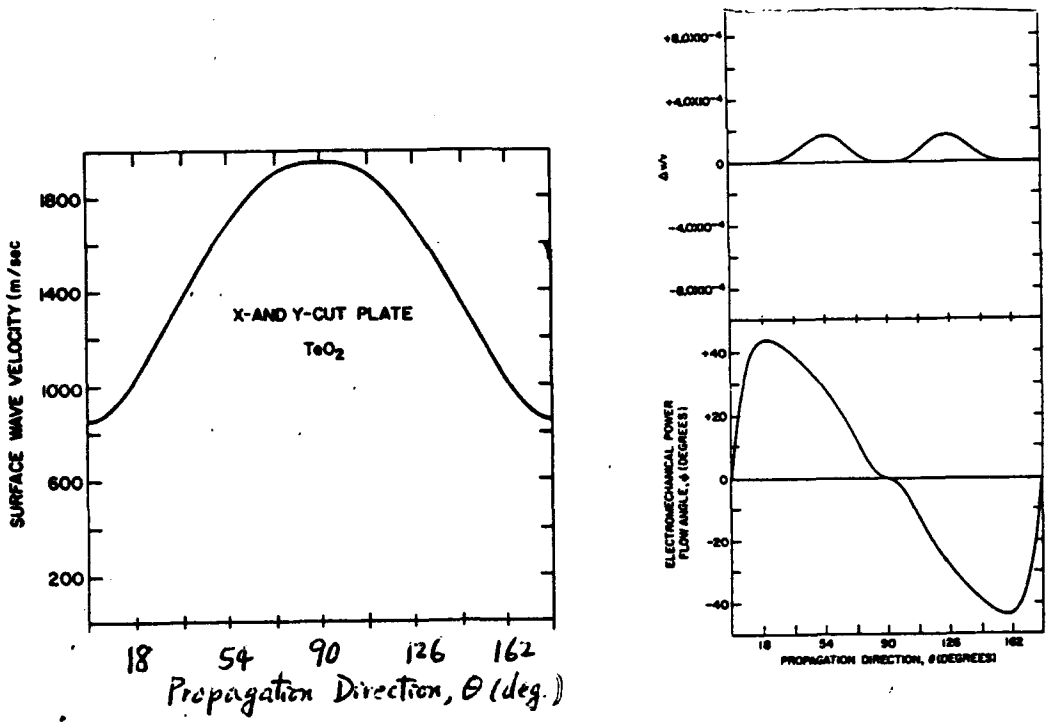

Figure 3, Velocity, ΔV/V, and Power Flow for Surface Acoustic Wave on (100) Cut TeO2.

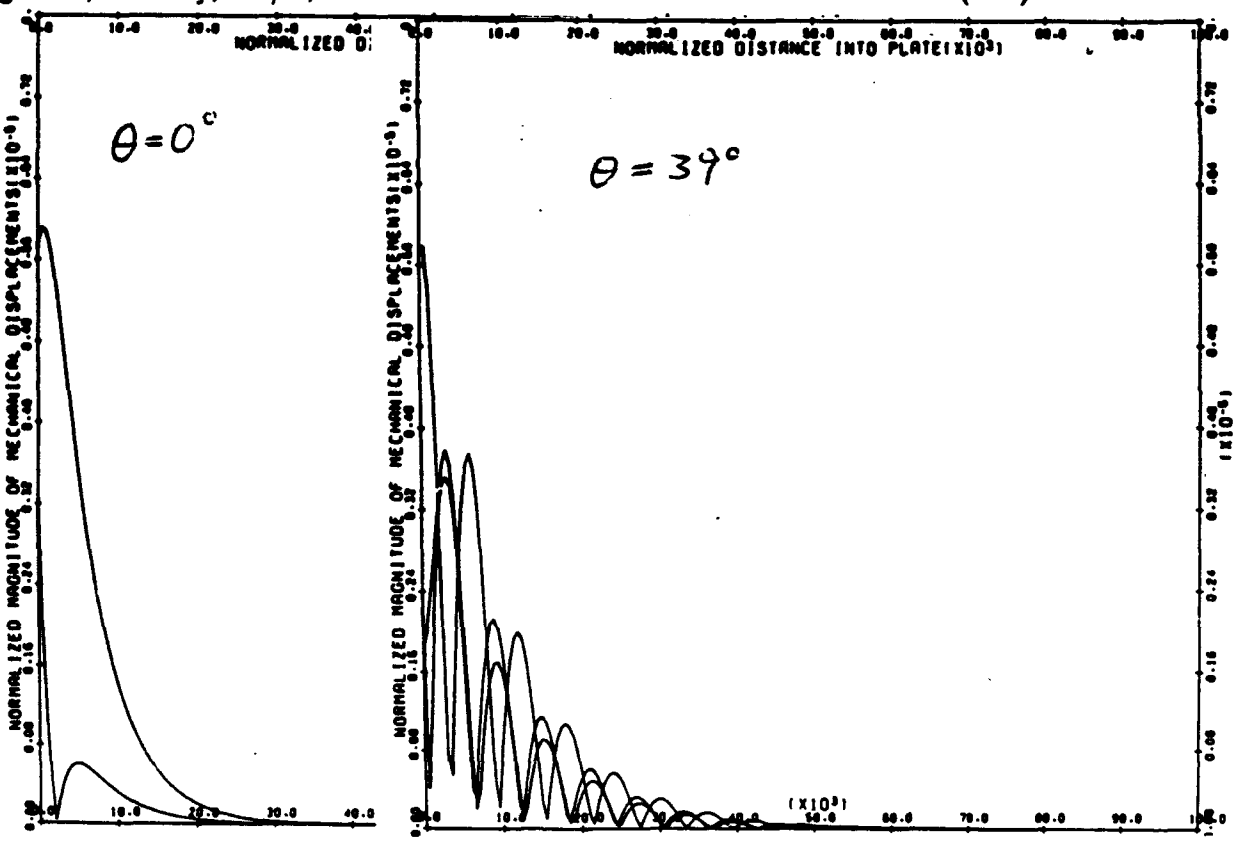

Figure 4, Particle Motion for SAW on X or Y Cut Plates.

2.1.2. REVIEW OF KNOWN TeO_2 SAW DATA:

At this point, there is no doubt about the validity of the PC based computer model and the accuracy of the material parameters used in the model. Figures 1 to 8 represents practically all was known in the open literature about surface acoustic wave properties on TeO_2. In these figures, for the sake of simplicity, the particle displacement distribution data is given only for the most interesting point of the velocity curve for a particular cut. In those early dates, researchers were looking for zero temperature coefficient cuts, which TeO_2 has, with large electro-mechanical coupling constants, which TeO_2 does not have. 4-6

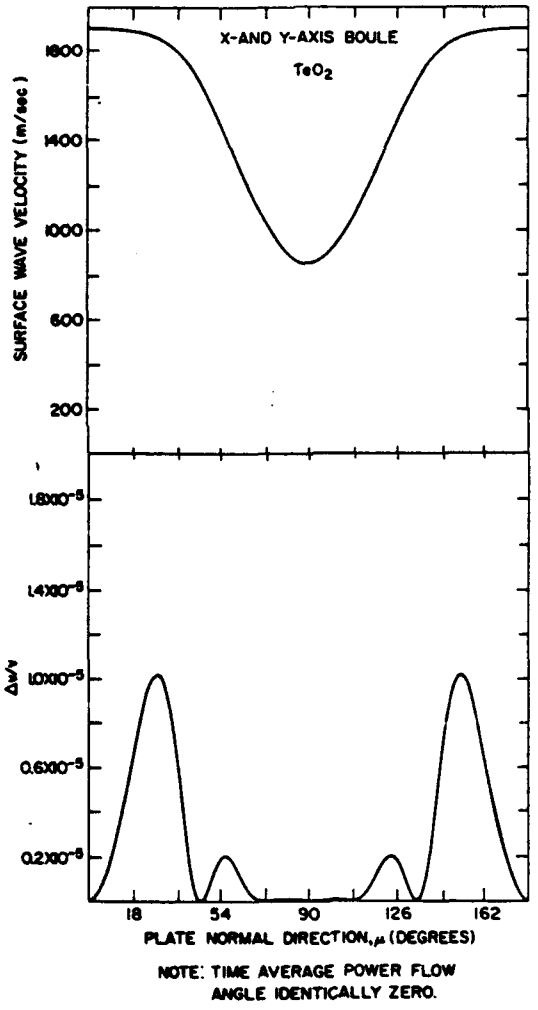

Figure 5, Velocity, ΔV/V, for SAW on X Cut Boule.

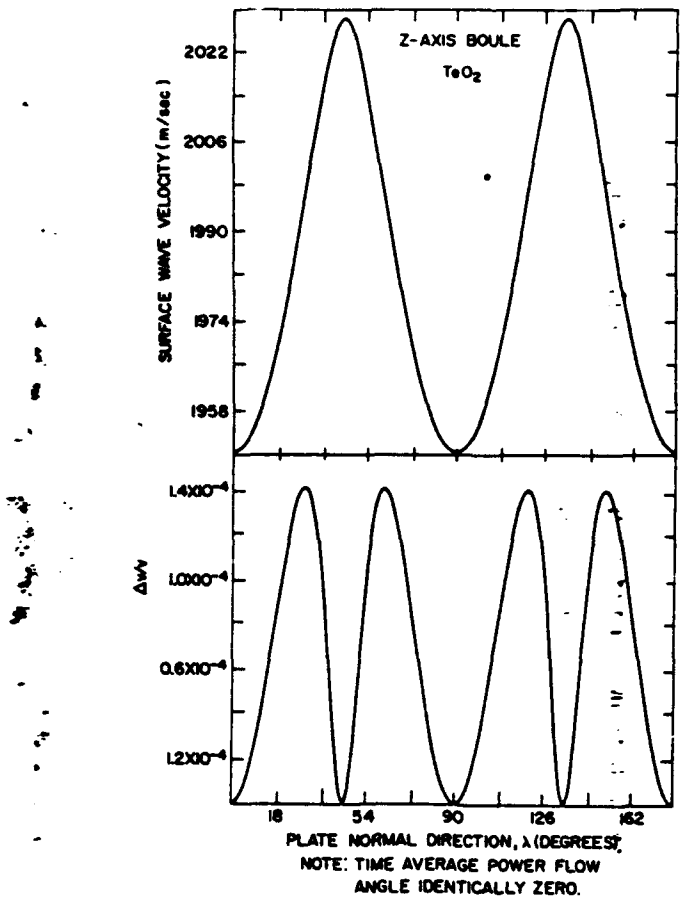

Figure 6, Velocity, ΔV/V, for SAW on Z Cut Boule.

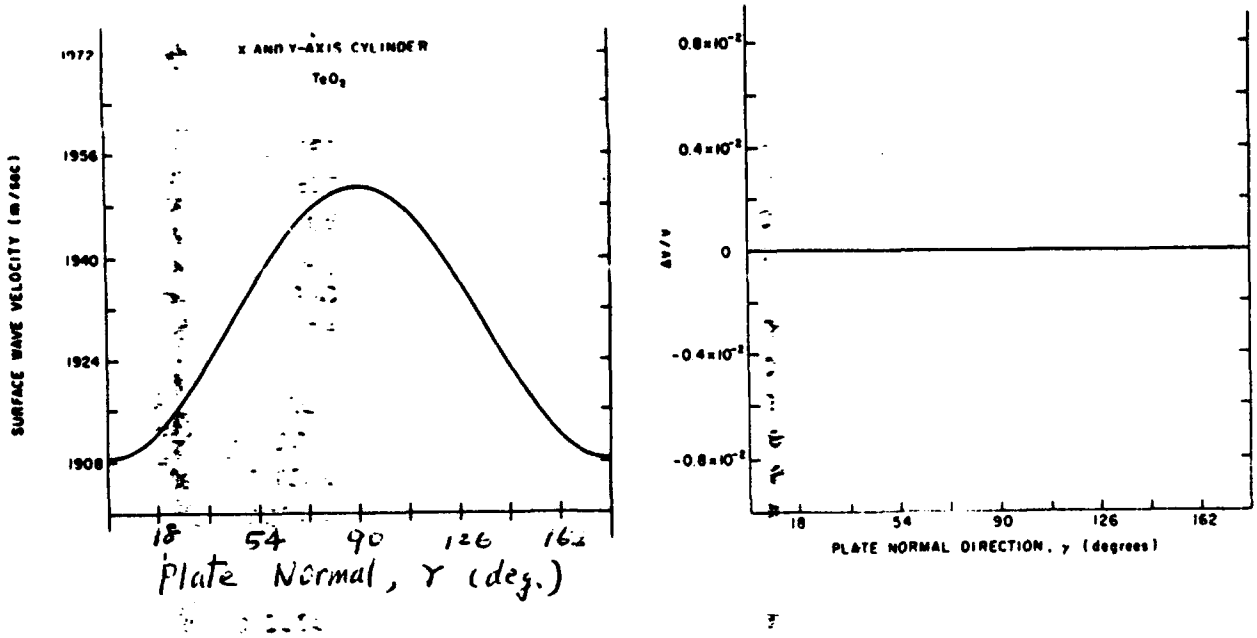

Figure 7, Velocity, ΔV/V, for SAW on X Cut Cylinders.

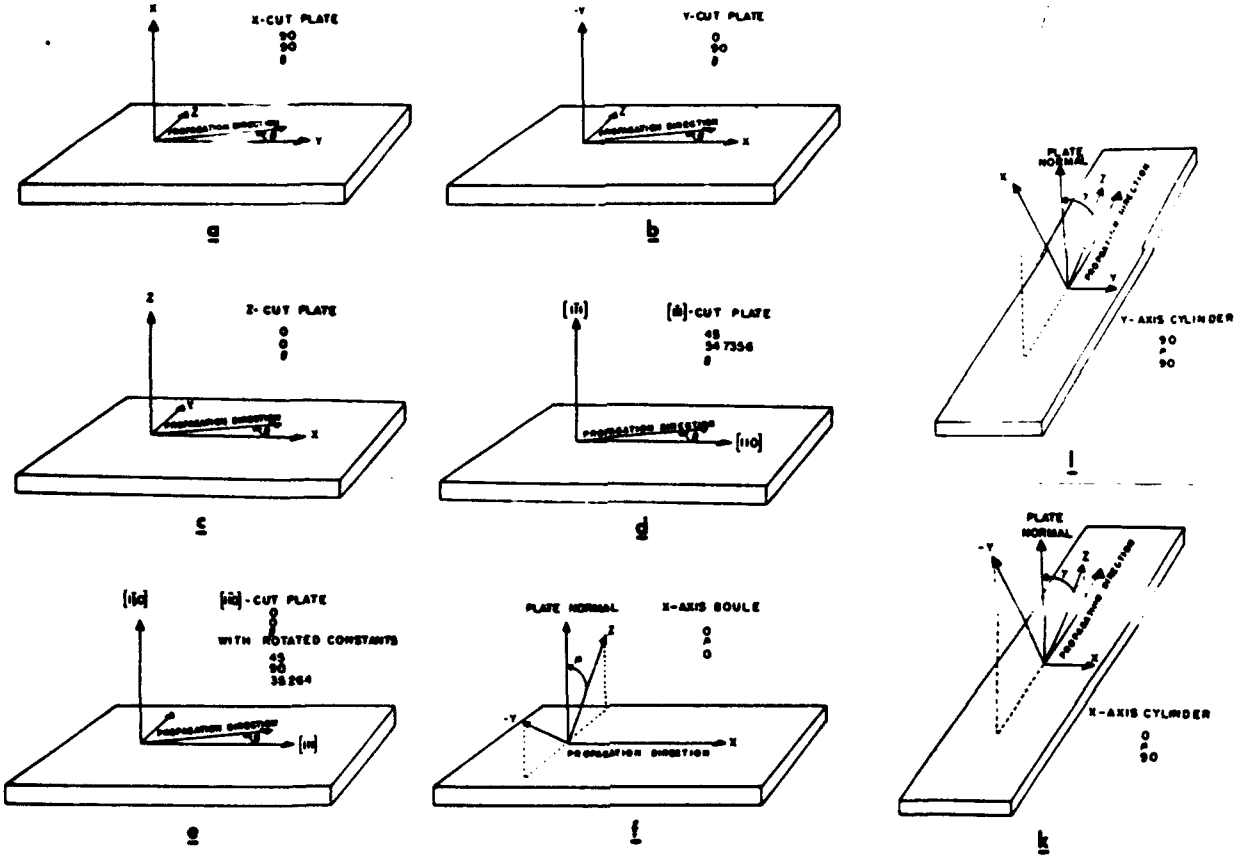

Figure 8, Definition of Cuts, Boule, and Cylinder.

These figures represent rather extensive work of surface acoustic wave data on x, y, and z cut plates (with varying propagation direction), of x, y, and z cut boule (with constant propagation direction but rotating the plate surface about the propagation direction as axis), and of x, and y cylinders (with varying propagation direction and plate surface simultaneously, rotating about an axis on the substrate but perpendicular to the propagation direction). Several cuts were found to support slow surface wave velocities around 0.84 mm/μs. Such slow surface wave velocity is slower than any other well known surface acoustic waves to date, but is almost 40% faster than the slow shear bulk wave in TeO_2 along the <110> direction. The z-cut plate does show a trend for the surface acoustic velocity to go down to 0.61 mm/μs at the <110> direction although the surface acoustic wave can not be supported at <110> and thus become bulk wave instead.

For the objective of this phase I program, the prospect does not seem very promising at this point. Note that (1) along the slow bulk wave direction <110>, the slow surface wave can not be supported, (2) the $\Delta V/V$, a measure of piezoelectric coupling constant, is very low in general, and becomes zero at the slow wave direction, (3) the surface acoustic field distribution sometime become oscillatory making efficient acousto-optic interaction tricky. One may be forced to use a faster acoustic surface wave at oblique angles of z-cut plate, or at either x or y cut <110> propagation, or at (110) cut x or y

propagation, or to hope for a useful slow surface skimmy wave (or shallow bulk wave).

2.1.3. SAW DATA ON (-110) CUT OF TeO_2 :

The computer program is used extensively to search for a slow acoustic surface waves. Particular attention is paid to the (-110) cut <110> propagation direction which is pretty much the only hope for finding a slow surface acoustic velocity comparable to the <110> slow shear bulk wave. The calculated SAW velocity surface is given by figure 9.

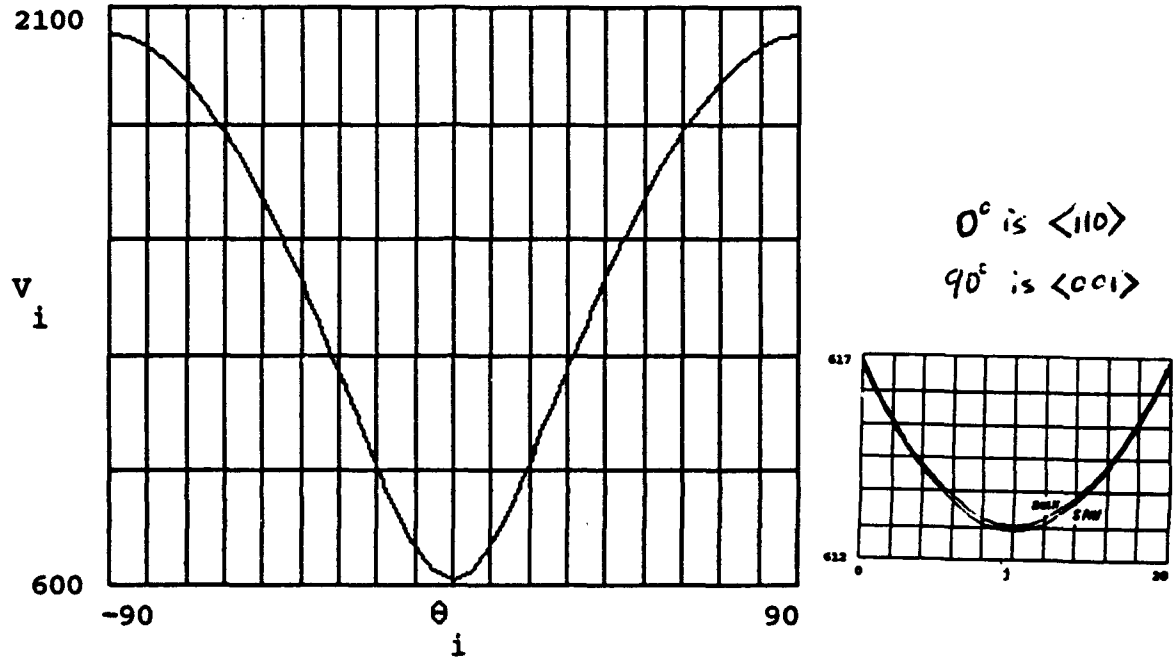

Figure 9, SAW Velocity Surface on ($\bar{1}10$) Cut TeO_2 Plates.

From figure 9 it is noticed that a slow SAW do exist along the <110> propagation direction on the (-110) cut (note the four fold symmetry of TeO_2 making <110> and <-110> equivalent). Figure 9 also compares the SAW velocity to the slow shear bulk wave velocity in the vicinity of the <110> direction. This slow surface wave follows the slow shear bulk wave extremely closely on the (-110) plane. The slow SAW velocity is 0.6128 mm/μs, only very slightly slower than the velocity of the slow shear bulk wave, 0.6129 mm/μs calculated by the PC based computer model. Note that the observed slow shear bulk wave velocity is 0.616 mm/μs such small difference is not unusual. The very small difference between SAW and slow shear bulk wave velocities is reason to worry about the validity of the slow SAW.

Generally, the SAW velocity must be slower than all bulk waves propagating along the

same direction otherwise the SAW will be converted to bulk wave components that has slower velocity than the SAW, and its power will be radiated away from the surface as it propagates. That is why the very close velocity values of the slow SAW and the slow shear bulk wave along <110> is worrisome, particularly when earlier published data for SAW along <110> on (001) cut TeO_2 is slow but not supported. One good sign is that this PC based computer model also predicts an unsupported slow SAW on (001) cut TeO_2.

To find out a little more about the validity of this slow SAW, data were compiled for SAW velocity versus slow shear bulk velocity on the <110> boule as shown by figure 10. At zero degree is the (-110) cut and at 90 degree is the (001) cut. Note that the slow SAW velocity becomes faster than the slow shear bulk wave velocity beyond 60 degree. This curve predicts a range of slow SAW existence in agreement with known data. Thus, it is strongly believed that the slow SAW probably do exist on the (-110) cut TeO_2. Ultimate answer to the existence question must be found experimentally.

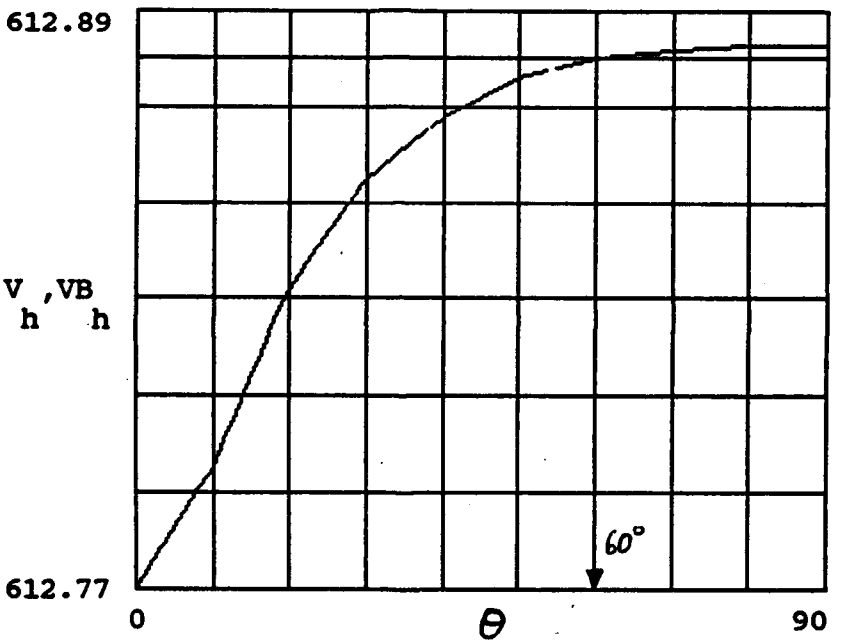

Figure 10, Comparison Between Slow SAW and Slow Shear Bulk Wave Velocities on (-110) cut Boule of TeO_2.

2.1.4. PROPERTIES OF THE SLOW SAW:

It is very interesting to find a supported slow surface acoustic wave along the <110> direction of the (-110) cut TeO_2 substrate. Note that this is the same direction as the famous slow shear bulk wave in TeO_2. The surface acoustic wave velocity calculated is 0.6128 mm/μs which is only 0.02% slower than the calculated slow shear wave velocity of 0.6129 mm/μs. Figure 11 gives the field distribution (amplitude) into the thickness

of TeO2 substrate. Note that the <110> component (shear) of SAW field penetrates as deep as 42 wavelengths (half amplitude point) into the substrate, a very unusual behavior since typical surface acoustic field only exist in the first one wavelength under the surface. On the other hand, the <-110> component (longitudinal) of SAW field decays within 0.02 SAW wavelength from the surface.

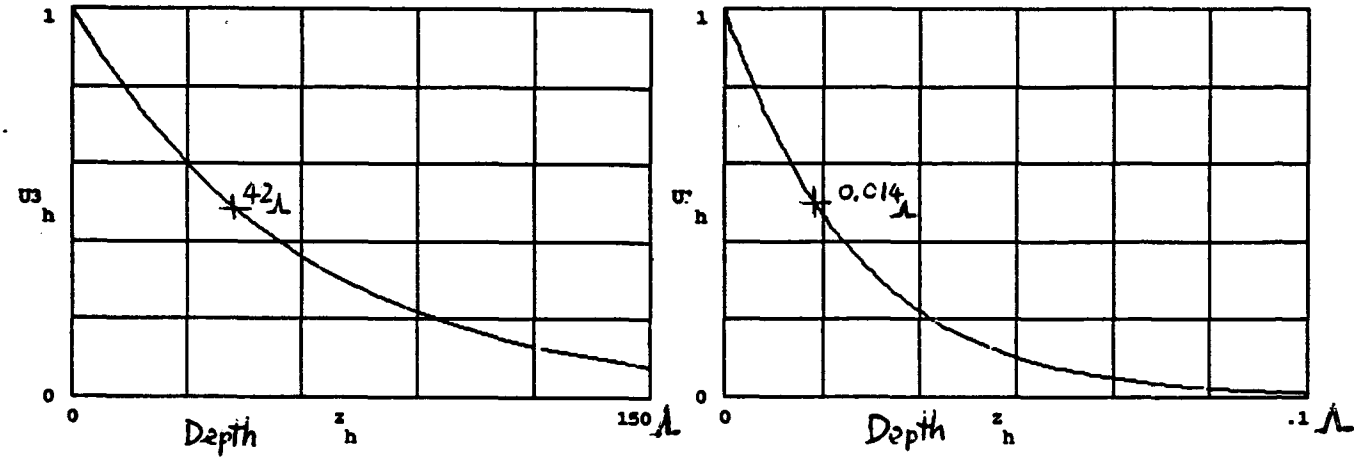

Figure 11, Field (Particle Displacement) Distribution for the Slow SAW.

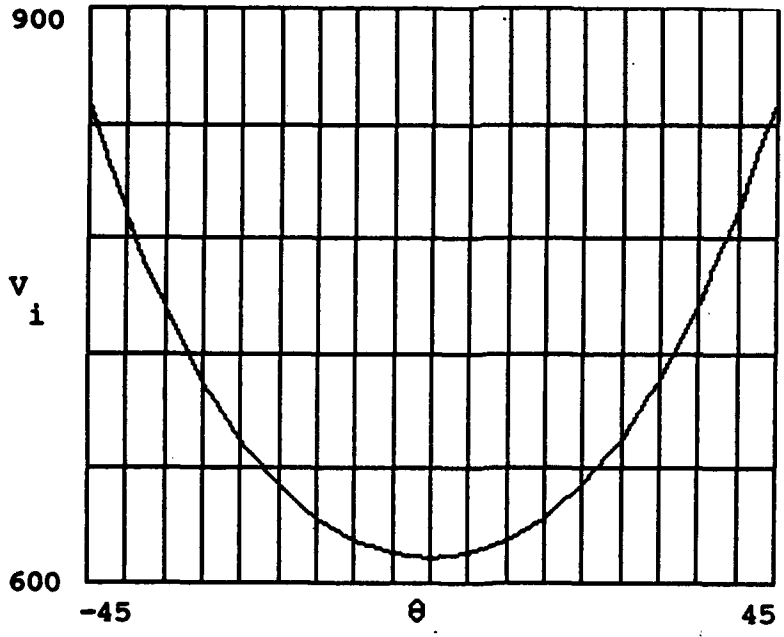

Figure 12, Slow SAW Velocity Curve for Z-Axis Cylinder of TeO2.

The calculated acoustic field distribution also indicates the dominance of the slow <110> shear vector component, which amounts to over 98% of the acoustic intensity even on the very surface of substrate where the <001> longitudinal vector component is highest. This property is considered advantageous for SAW interaction with focused laser beams.

The slow shear bulk wave is well known for its extremely large anisotropic properties in the (001) plane and in the (-110) plane. The huge anisotropic properties require precision crystal orientation during slow shear wave device fabrication. The concern is in precision orientation requirements for the slow SAW. Figure 12 gives the slow SAW velocity curve for z-axis cylinder of TeO_2. It is interesting to note that the SAW velocity variation in the z-axis cylinder is much smaller than the anisotropy of slow shear bulk wave in the z-plane, see figure 13.

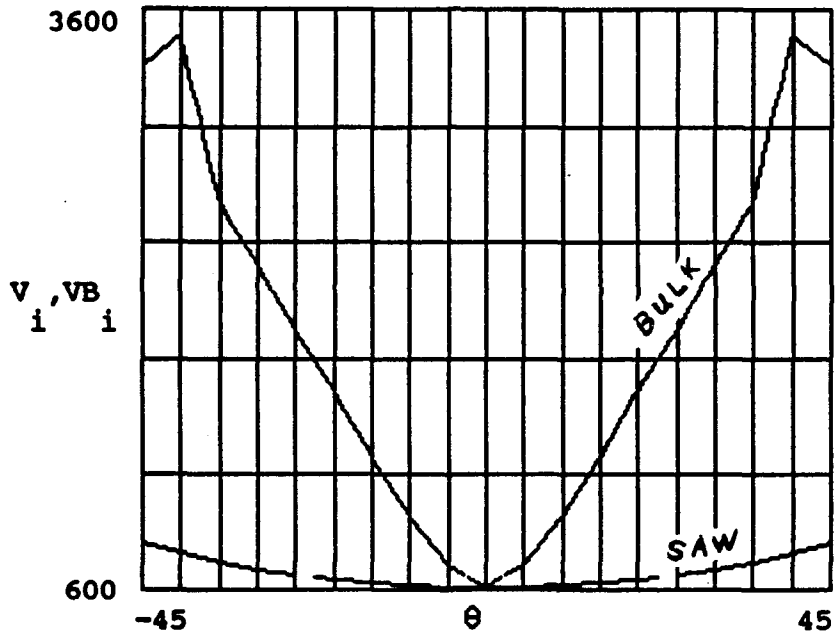

Figure 13, Comparison of Slow SAW and Slow Shear Bulk Wave Velocities in the Z-Cylinder and in the Z-Plane Respectively.

In summary, it is exciting to find a slow SAW along the <110> direction of (-110) cut TeO_2 substrate. This slow SAW has lots of similarity with the slow shear bulk wave in the same direction. In fact, the majority of the slow SAW power is carried in the shear vector component parallel to the slow shear bulk wave. The slow SAW has similar huge anisotropy on the (-110) plane, but is rather tolerant to crystal surface orientation error (the angle between surface normal and <-110>). An important property of the slow

SAW is the unusually deep penetration of its shear component into the thickness of substrate, about 42 wavelengths for half amplitude point. The deep shear field will be beneficial for surface acousto-optic interaction with free propagating focused laser beams.

2.2. SAW LAUNCHING TECHNIQUES:

2.2.1. DIRECT GENERATION OF SURFACE WAVE ON TeO_2 :

Surface acoustic waves can be generated on certain directions of piezoelectrical substrate using interdigital transducer electrodes. TeO_2 is a piezoelectric crystal. Its electro-mechanical coupling constant has been calculated by Slobodnik et. al. in the form of $\Delta v/v$, where v is the surface acoustic wave velocity and Δv is the change in surface acoustic wave velocity due to the application of a conductive plane on the substrate surface. The coupling constant, k^2, equals 2 times $\Delta v/v$. Figure 3 shows some of the computed results.

Note that the electro-mechanical coupling constant is about 0.003, which means optimal interdigital transducer will have 17 finger pairs and will offer only 6% fractional bandwidth. Reduce the number of finger pairs increases the bandwidth with the penalty of insertion loss. In addition, the electro-mechanical coupling constant vanishes at the surface acoustic wave velocity minimum directions where our interest is highest. In any case, the electro-mechanical coupling constant is too small for most acousto-optic signal processing applications which usually demands wideband. The small coupling constant require the generation of surface acoustic waves using techniques external to the TeO_2 substrate.

2.2.2. OTHER REPORTED SAW LAUNCHING TECHNIQUES:

Many techniques for the generation of surface acoustic waves on non-piezoelectric substrate has been investigated before.[7-11] These include bulk to surface acoustic wave converters such as prism couplers, grating couplers, and reflective couplers, see figure 14.

Deposition of piezoelectrical thin film such as (001) oriented ZnO or PZT film can be very useful too. Several basic versions of thin film SAW transducers exist as shown by figure 15. The top electrode version usually uses the first peak of the general coupling curve has a relatively smaller $\Delta v/v$ value. However, the requirement of very thin deposited piezoelectric layer helps to minimize the problems of acoustic propagation loss and mode conversion as the acoustic wave transits from a layered structure to uncoated substrate surface area.

Edge bonded transducers[12-13] can provide very broad bandwidth with high conversion efficiency although the fabrication is not the easiest. Flip chip coupling can be a simple and easy way for laboratory explorations although the configuration is not ruggedized

enough for incorporation into applications. These approaches are illustrated by figure 16.

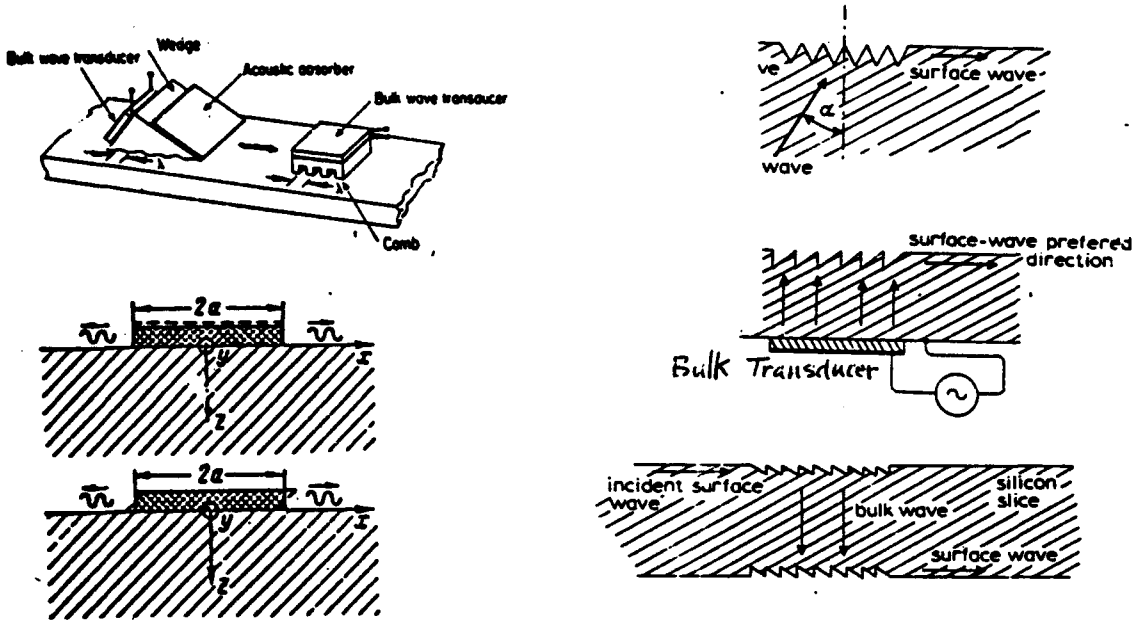

Figure 14, Bulk to Surface Acoustic Wave Conversion Means.

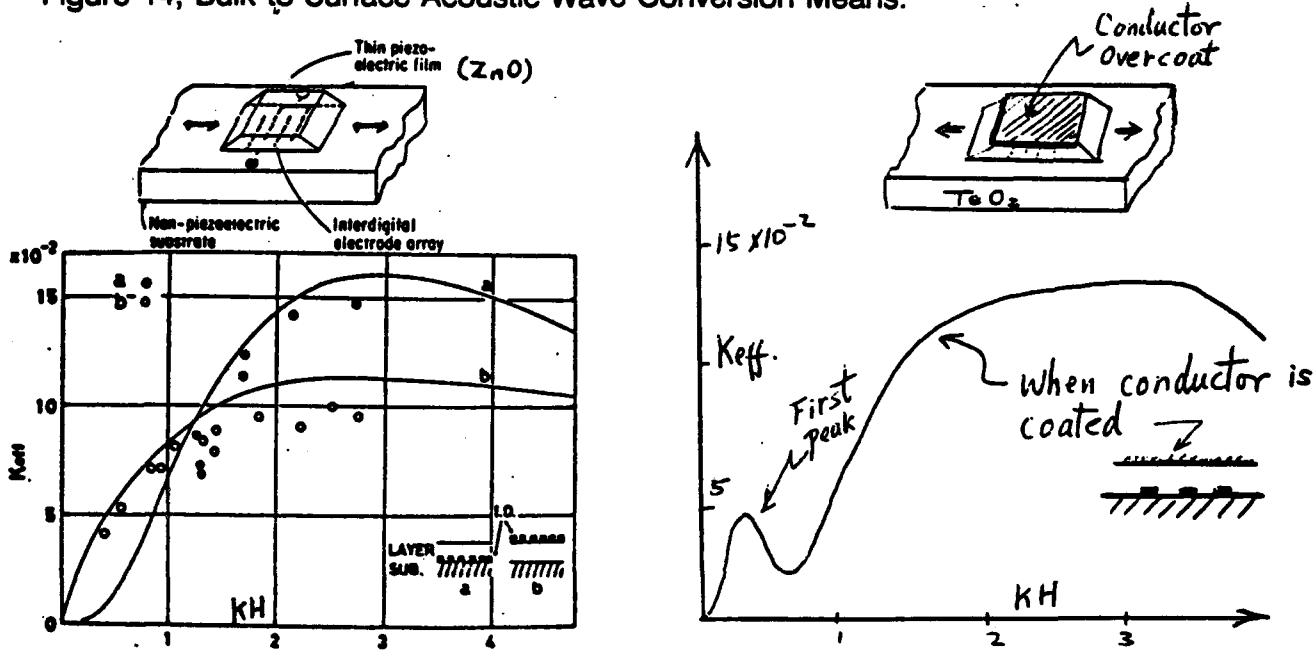

Figure 15, Conversion Efficiency for Several Configurations of Thin Film SAW Transducers.

2.2.3. SURFACE ACOUSTIC WAVE LAUNCHING COMPARISON:

The suitability of these very different approaches for the present application is briefly compared here. The deposited ZnO transducer has a coupling constant of 0.02 at best. [7, 11] Optimal transducer requires 7 finger pairs and offers 15% bandwidth. The requirement of 30% bandwidth must be provided with two transducers[4] or must be traded with conversion loss. The edge bonded transducer using $LiNbO_3$ platelet or ZnO can easily meet the 30% bandwidth requirement with low loss. But it is difficult to fabricate as multiple transducers at different propagation directions as required by the army. The corrugated surface bulk to SAW converter is interesting as it has the potential of offering both bandwidth and efficiency. However, it has not been fully developed and may have some hidden problems.

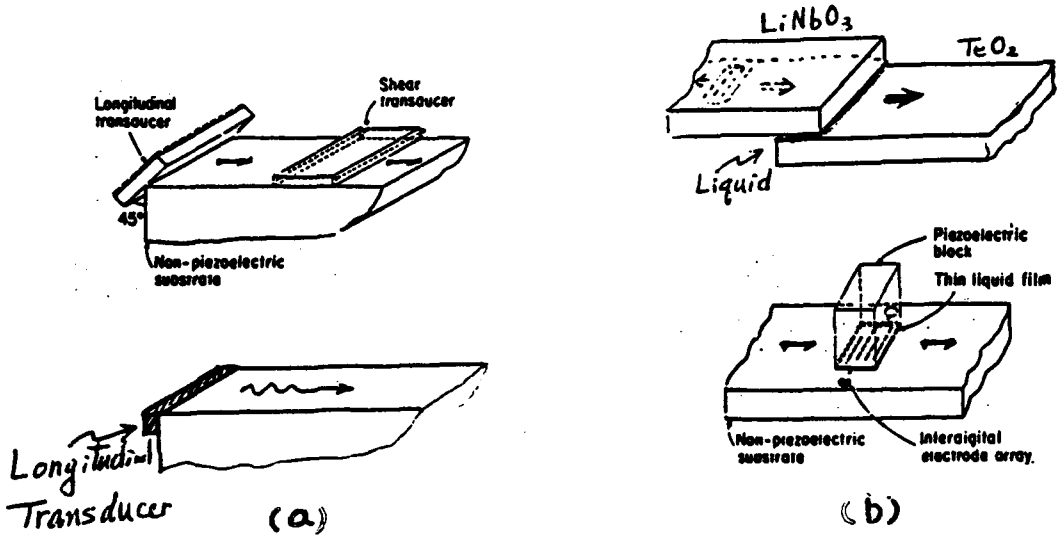

Figure 16, (a) Edge Bonded Transducer and (b) Flip Chip Coupler.

A new SAW launching method is devised for this newly found slow SAW on TeO_2 as shown by figure 17. The new method take advantage of the deep acoustic field of the slow SAW by reflecting a slow shear bulk wave column towards the (-110) crystal surface. This method has the advantage of easier transducer fabrication and launching the slow SAW at middle of a substrate by etching deep V-grooves.

In summary, the most promising slow SAW launching methods are the edge-bonded transducers and the reflection bulk to SAW converter. For the experimental observation of the slow SAW, the bonding of acoustic transducers can be replaced by glued bonding at lower acoustic frequencies. In such cases, the glue thickness needs be thin comparing to the acoustic wavelength in the glue. Frequencies lower than about 30 MHz for shear waves will be adequate. For real applications, the transducers need to be metal bonded to minimize the conversion loss and maximize the bandwidth. Such transducers will be

able to provide efficient electro-mechanical conversion with octave bandwidth.

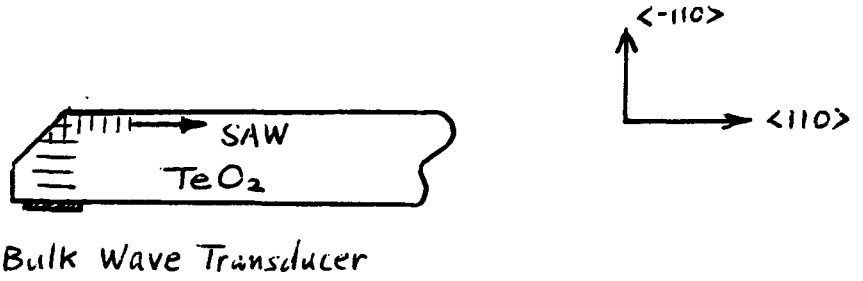

Figure 17, New SAW Launching Method for the Slow SAW on TeO2.

2.3. SAW INTERACTION WITH LASER BEAMS:

2.3.1. SURFACE ACOUSTO-OPTIC INTERACTION :

From figure 9, we notice the slow SAW velocity in the vicinity of <110> direction is highly anisotropic. The slow SAW velocity is 0.6128 mm/μs, nearly identical to the slow shear wave. The acousto-optical figure of merit M_2 for the slow SAW is expected same as the slow shear wave as well since value of all constituents remain the same and since the longitudinal component of the slow SAW is negligible. However, the interaction geometry between the slow SAW and a laser beam can be different from that of conventional bulk wave acousto-optic devices. Often the laser beam will be focused and bouncing off the under side of the substrate surface by total internal reflection. The attention of this section will be dealing with the surface acousto-optic interaction.

For a laser beam, which passes through the subsurface region with total internal reflection from the surface, the interaction is the integration over the depth of the surface acoustic field. Computation of the overlap integral between the optical field and acoustic field gives the interaction as function of acoustic frequencies. The deep acoustic field of the slow SAW on TeO2 will be beneficial for surface acousto-optic interaction.

To calculate the surface acousto-optical interaction, one needs to calculate the induced refractive indices due to each stress component in the surface wave. Then, the induced refractive indices are applied to the optical field to obtain phase retardation. Due to the z dependence of the SAW stress and the oblique propagation of the optical beam

through the subsurface region, the effects must be integrated over the depth of the surface field.[13] The exact calculation can be rather involved, a simplified calculation procedure is given as follows.

Let the acoustic stress field be represented by the six element vector $[S_j(z)]$, the abbreviated photo-elastic tensor be represented by the 6 x 6 matrix $[P_{ij}]$, the induced refractive indices is given by $[N_i(z)]$, which has six components.

$$[N_i(z)] = [P_{ij}] * [S_j] \qquad (1)$$

and

$$\int [N_i(z)\, dz \overset{\Delta}{=} [NI_i(z)] \qquad (2)$$

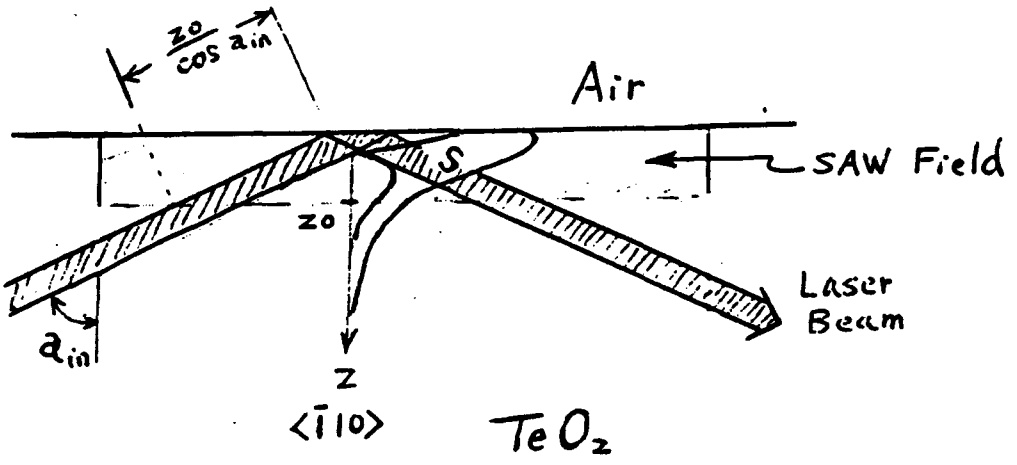

Figure 18, Overlap Between A Collimated Laser Beam And Saw Field.

Assuming the interaction length is shorter than the depth of focus of the laser beam, the overlap integration between the acoustic and optical fields may be simplified by the model of figure 18. The average induced refractive indices seen by a pencil ray is given by the integral function of the induced refractive indices, $[NI_i(z)]$, divide by a round trip distance over the stress field depth,2*zo. The application of the average induced refractive indices to rays entering and exiting the acoustic field depends on the geometry of incidence angle and acoustic beam width. For figure 18, the acoustic beam width is sufficiently large for maximum interaction, all optical rays shall enter the acoustic field from the bottom and shall travel through the entire acoustic field depth round trip. The effective induced refractive indices is the maximum value, $2*[NI_i(zo)]$, for all optical rays.

The distance of travel under the influence of acoustic field, i.e. the acousto-optical interaction length, is thus $2*zo/\cos(\theta_{in})$, where θ_{in} is the angle of incidence to the edge of a 90 degree substrate edge. The optical phase retardation for each of the polarization component, i, is therefore, $2*[N_i(zo)]/\cos(\theta_{in})$. For θ_{in} approaching 90 degree, the laser beam will be parallel to the SAW surface and the phase retardation formula breaks down to infinity, the finite acoustic beam width becomes important. Interaction under such condition will be discussed in section 2.3.2.

The evaluation of equations (1) and (2) can be involved in general. However, for the slow SAW on TeO2, only one shear stress component is important and the evaluation of equation (1) is no longer needed. Integrating over the exponential decay field, equation (2), is all is needed.

2.3.2. GEOMETRIC FACTOR FOR SURFACE ACOUSTO-OPTIC INTERACTION:

In this section, the finite size of SAW beam width will be considered. The optical rays may enter the acoustic field from its edges or from the bottom depends on set-up parameters. Therefore, the interaction factor has to be calculated numerically. In general, the acousto-optic efficiency can be described by equation (3), where $L' = L \sin^{-1} \theta_{in}$,

$$\eta = \sin^2 \{ (\pi/\Lambda) [L'F] \sqrt{(M_2 P_d)} \} \qquad (3)$$

L is the acoustic beam width, P is the SAW power, P_d is the average SAW power density given by P/(L zo), Λ is the optical wavelength, and F is the integration of an arbitrary optical ray over the acoustic field. Note the sin factor in the definition of L' means that as the optical rays come in at oblique angles, the numerical integration must be carried out for longer optical path assuming the exponential tail of acoustic field extends to infinity. The dimension related parameters may be rearranged into a new factor, $G = F^2 L'^2 / (L\ zo)$, and equation (3) becomes

$$\eta = \sin^2 \{ (\pi/\Lambda) \sqrt{(M_2 P G)} \}$$

$$\approx (\pi/\Lambda)^2 M_2 (P G) \qquad (4)$$

In equation (4) the geometric factor, G, is an indication of the effectiveness of the surface acousto-optic interaction geometry. In comparison, the bulk wave counter part of G is simply (L/zo). The geometric factor, G, is the most important parameter to be calculated for evaluating surface acousto-optic devices. Figure 19 gives the geometric factor, G, versus normalized SAW beam width, L/zo the bulk wave geometric factor, with the optical incidence angle θ_{in} as parameter. As expected, at larger incidence angle, the factor G approaches unity. At smaller incidence angle, the optical rays goes in and out of the acoustic field rather quickly. Thus, longer acoustic beam width, L/zo, may even cause the geometric factor to decrease. For small values of L, the value of G increases in proportion to (L/zo). Eventually (L/zo) becomes too big and the G factor falls off.

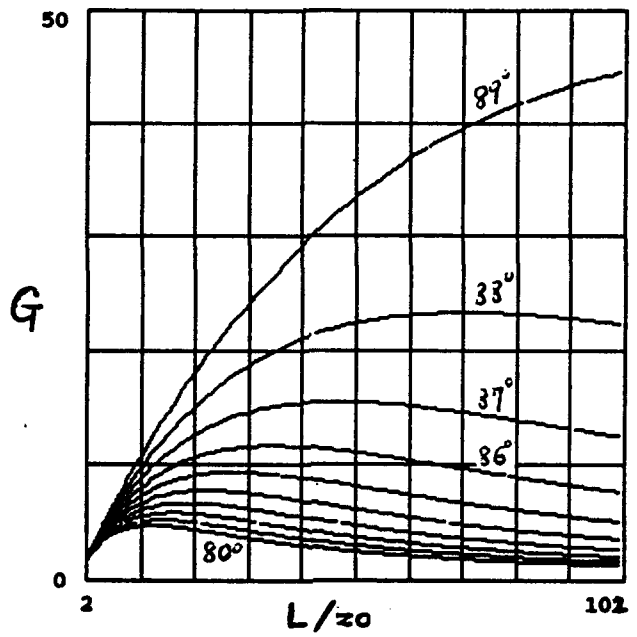

Figure 19, Surface AO Geometric Factor, G, versus Acoustic Beam Width, L/zo, for Optical Rays Reflecting at Center of Acoustic Beam with Optical Incedence Angle as Parameter.

Figures 20 to 23 give the geometric factor, G, versus L/zo with x/zo, the normalized off-set distance from center of the acoustic beam, as parameter. Each figure corresponds to an optical incidence angle. In these figures it is clear that there is an optimal value of (L/zo) for each optical incidence angle. The effect of off-set distance, x, becomes more important as the incidence angle increases.

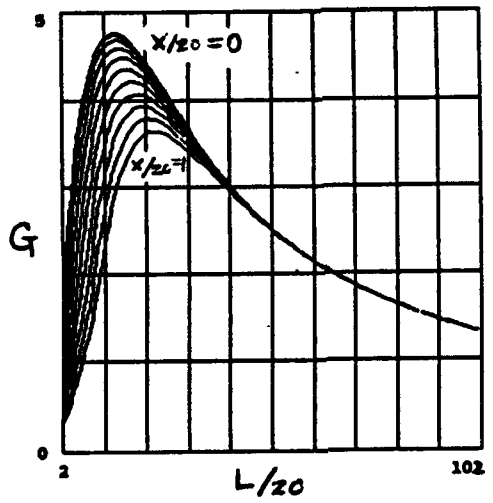

Figure 20, Surface AO Geometric Factor, G, versus L/zo for Optical Incidence Angle of 80 degree with Off-Set Distance, x/zo, from Beam Center as Parameter.

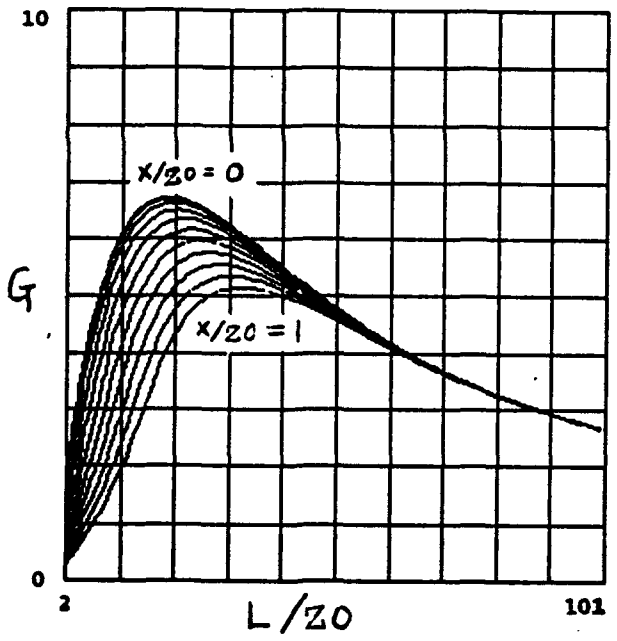

Figure 21, Surface AO Geometric Factor, G, versus L/zo for Optical Incidence Angle of 83 degree with Off-Set Distance, x/zo, from Beam Center as Parameter.

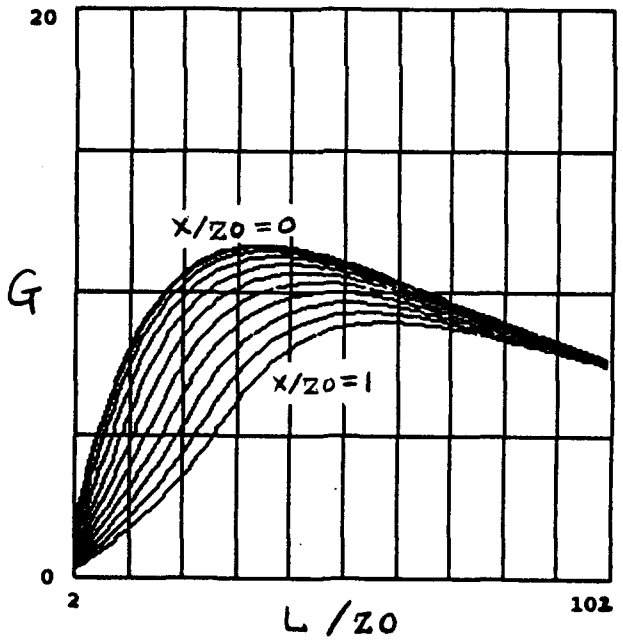

Figure 22, Surface AO Geometric Factor, G, versus L/zo for Optical Incidence Angle of 86 degree with Off-Set Distance, x/zo, from Beam Center as Parameter.

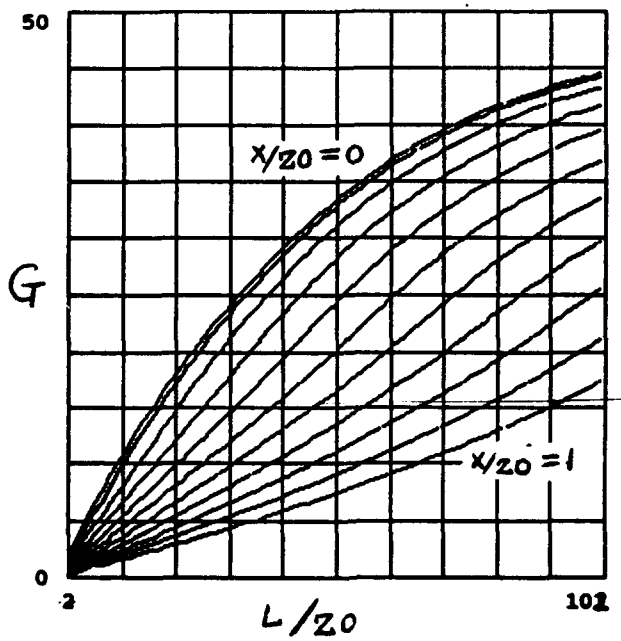

Figure 23, Surface AO Geometric Factor, G, versus L/zo for Optical Incidence Angle of 89 degree with Off-Set Distance, x/zo, from Beam Center as Parameter.

In the above figures the optical input are rays of zero width. In reality, optical beams have finite beam width and divergence angle. Assuming the acousto-optic interaction range is shorter than the depth of focus of laser beam, the effect of finite optical beam width can be handled by integration over the off-set parameter x with a gaussian weighing factor.

In summary, the acousto-optic interaction with the slow SAW is relatively simple due to only one dominant particle displacement vector in the slow SAW field. The interaction between the total internally reflected laser beam and the exponential decay SAW field into the thickness of the substrate requires a geometric factor, G, which has been calculated with varying values of normalized acoustic beam width , L/zo, normalized off-set displacement value from center of the acoustic field, x/zo, and optical incidence angle, θ_{in}. The surface acousto-optics geometric factor, G, approaches the geometric factor for bulk acousto-optics, L/zo, when the acoustic width, L, is small or when the incidence angle, θ_{in}, approaches 90 degree. Therefore, in designing efficient surface acousto-optic spatial light modulators, one must determine the optical incidence angle, optical beam size, and the acoustic wavelength related field penetration parameter, zo, before designing the transducer width, L. The large field penetration depth for the slow SAW is advantageous for surface acousto-optic interactions in keeping L/zo small.

2.4. EXPERIMENTAL RESULTS:

Experimental observation of the slow SAW is very important since it has never been reported before, and since there is some doubt about the existence due to the velocity being so close to the slow shear bulk wave. Equally important is verification of the unique properties of this slow SAW on (-110) TeO_2, notably its deep penetration depth, its slow velocity, and its large M_2 value similar to that of the slow shear wave.

2.4.1. GENERATION OF <110> SAW ON (-110) CUT TeO_2:

A shear wave transducer operating between 18 to 40 MHz is bonded to the edge of a (-110) cut TeO_2 crystal of 5mm x 5mm x 30mm. The orientation of the crystal is (001), (110) and (-110), a standard slow shear bulk wave cut with 30mm along the <110> direction. The crystal edges are carefully polished to orientation in the <110> direction within 5 minute, and to retain a sharp edge so as to allow the bonding of acoustic transducer all the way to the edge. The orientation of the (-110) surface is not particularly critical and is deemed within 10 minutes. The transducer is made of a section of a shear wave fused quartz Q-switch. The transducer of the Q-switch resonance frequency is about 19 MHz. Top electrode of the Q-switch section has been re-deposited and is 8mm by 2mm. The Q-switch transducer is glued by thin epoxy layer to the 5mm x 5mm end of the TeO_2 crystal with half of its top electrode (1mm by 5mm) overlapping the TeO_2 as shown by figure 24. The polarization of the transducer is oriented along the <-110> direction, a very important point. The exposed portion of top electrode allows attachment of wiring by silver paste.

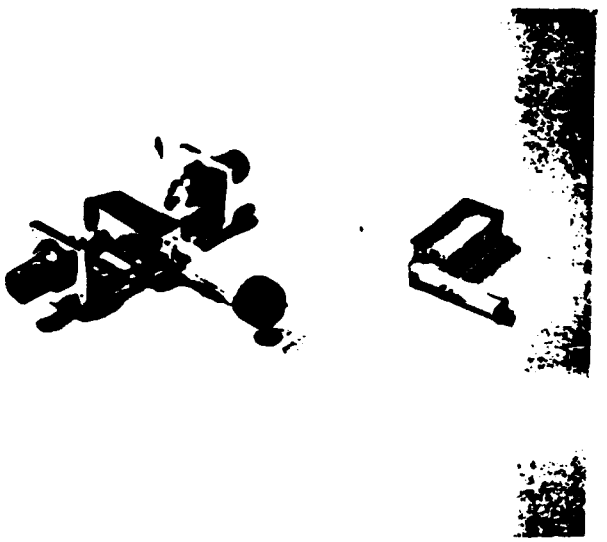

Figure 24, The Experimental Device for Observation of Slow SAW on TeO_2.

The experimental sample is mounted on a metal holder with RF connector and is driven by up to 300 mW of RF from a sweep oscillator. It should be noted that the double side loading of the shear wave Q-sw transducer makes it extremely broadband. However, the acoustic wave generated will travel to both the fused quartz side and the TeO_2 side simultaneously with more in the fused quartz due to better quality of indium bond. Therefore, it is estimated that no more than 10% of the RF drive power will be converted to any kind of acoustic wave in the TeO_2. Exactly how much is in the slow SAW depends on the drive frequency. At the low frequency end, about 15 MHz, the depth of SAW field is estimated 1mm (half power point) and practically all acoustic power launched into the TeO_2 shall be in the slow SAW. At higher frequencies, increasing amount of launched power will be in the shear bulk wave and spurious response is expected.

2.4.2. OBSERVATION OF SLOW SAW ON (-110) TeO_2:

Observation of the acoustic surface wave and the residual bulk shear waves is made using the schilearin method. Measurements are made in terms of acoustic velocity, acoustic field depth into the crystal, and the acoustic frequency dependence of the field penetration depth. The transducer is excited at its fundamental frequency and at its overtone harmonic frequencies covering a frequency range from 15 MHz to 80 MHz.

In the first experiment, an expanded HeNe laser beam is allowed to pass through the crystal while a CW RF signal is applied to the acoustic transducer. The shear bulk wave generated by the acoustic transducer near the crystal surface will be converted to surface acoustic wave and certain amount of residual bulk waves. The bulk wave components shall lose its intensities rapidly because of Poynting vector walk-off due to the extraordinarily large acoustic anisotropy of the slow shear wave in TeO_2. On the other hand, the surface acoustic wave component shall be guided along the crystal surface not affected by the slow shear wave anisotropy on the (001) plane. After leaving the near field of the acoustic transducer, the slow SAW and the slow shear bulk wave shall be separated. The expanded HeNe laser beam will be diffracted by either the slow shear wave or the surface acoustic wave. When the diffracted optical components are separated from the undiffracted, image of the entire acoustic fields can be obtained by projecting the diffracted optical components onto a screen.

Observing the image of the acoustic field reveals a strong acoustic component near the surface of the crystal and propagating down the entire length of the 30 mm long crystal. For an effective acoustic transducer height of 1 mm, an acoustic wavelength of 23.5 micron at 26 MHz, the near field distance of the slow shear wave is only about 0.85 mm due to the large poynting vector walk-off angle in anisotropic medium. Therefore, the strong acoustic field component along the entire 30 mm length of the crystal surface can only be due to the surface acoustic wave.

The first side lobe of the slow shear wavefront shall have a phase vector tilted about 1.34 degree from the transducer normal. With the huge acoustic anisotropy, the Poynting

vector of the first side lobe shall be walking-off at an angle of about 60 degree. Indeed, we have observed the rapid departure of the first side lobe at near 60 degree from the transducer bonded crystal surface. The intensity of the sidelobe components get stronger as the drive frequency goes up indicating poorer coupling into the slow SAW as expected. The sidelobes reaches crystal edges rather rapidly and bounces in the crystal showing a Zig-Zag path disturbing experimental observation at high frequencies. Thus, most data collection were done at the low frequency end. Figure 25 illustrates the observed acoustic field distribution when the laser probe scans the crystal.

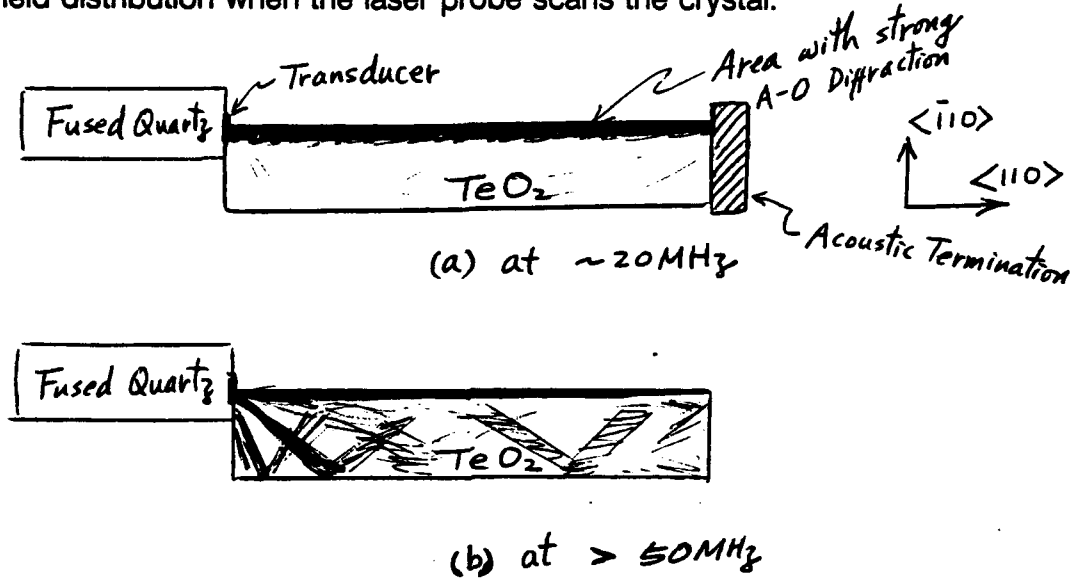

Figure 25, Observed Distribution of Slow SAW Field in (-110) cut TeO2.

2.4.3. MEASUREMENT OF THE SLOW SAW VELOCITY:

The surface acoustic wave velocity is measured using a focused HeNe laser probe beam traveling along the crystal surface. The acoustic transducer is driven by a modulated RF signal with fast rise and fall time allowing the measurement of delay time. The diffracted laser beam is intercepted by a fast photodetector and the detector output is monitored by an oscilloscope. The location of the laser probe beam is adjusted by mounting the crystal sample on an X-Y-Z translational stage. Time delays between the applied RF signal and the diffracted laser beam, and differential time delay between two probe beam locations are recorded. The delay time as well as differential delay time between two probe beam locations are measured repeatedly to improve the accuracy. The acoustic velocity is equal to the distance between probe beam locations divided by the differential time delay.

The average value of surface acoustic wave velocity measured is 613 m/sec which

is in excellent agreement with the theoretical number of 612.77 m/sec. Measured velocity within the first 5 mm from the acoustic transducer yielded a different acoustic velocity number of 615 m/sec which is between the published experimental slow shear velocity of 616 m/sec and the surface acoustic wave velocity. It is believed that the faster velocity observed in the vicinity of the acoustic transducer may be due to influences by the bulk slow shear wave components.

There is a dilemma that most people calculated slow shear bulk velocity to be 0.613 m/sec while published experimental slow shear velocity is 0.616 m/sec. So, why is the slow SAW velocity 613 m/sec instead of 615 m/sec. Presently due to limited number of samples measured, there is no answer to the question. The experimental accuracy should be better than 0.1% and most of the error is due to reading from the oscilloscope. However, the measured slow SAW velocity is in reasonably good agreement with analytical data, and is definitely slower than the velocity of slow shear bulk wave supporting the existence of slow SAW.

2.4.4. MEASUREMENT OF THE SLOW SAW FIELD PROFILE:

An interesting and unique feature of this slow surface acoustic wave along the <110> direction of (-110) TeO_2 is the deep acoustic field profile into the substrate. Typical surface acoustic waves only penetrate no more than a few acoustic wavelength into the substrate. However, our theoretical results for the slow surface acoustic wave on <110> direction of TeO_2 indicates that the slow SAW field will penetrate about 42 wavelength into the substrate, corresponding to the half amplitude point.

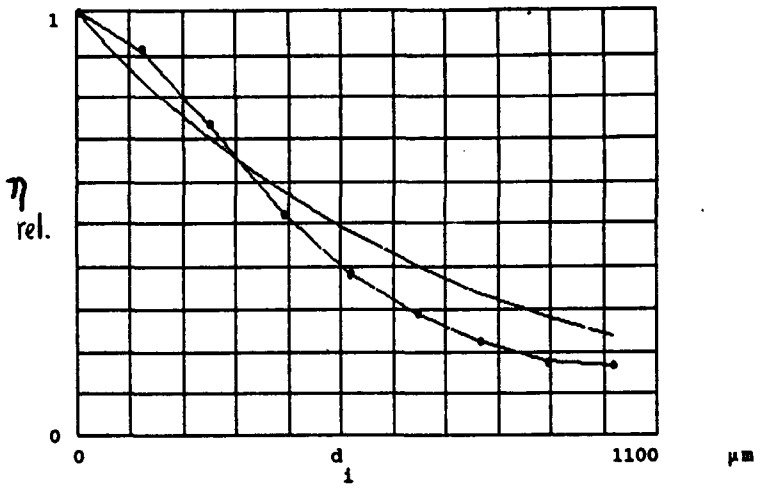

Figure 26, The relative diffraction efficiency of laser beam in the surface acoustic field of the crystal Teo2 as a function of the deepnees from the surface, vp=612.77 m/sec (theory), vp=613 m/sec (experiment) f=26 MHz, λ(laser)=0.6328 μm, P(laser)=3mW, distance between the tranducer and the measured point=7 mm

The surface acoustic field depth is measured also using the focused laser beam probe at 7 mm, 14 mm, and 21 mm away from the transducer. The laser probe is moved into the substrate gradually and the acousto-optical diffraction recorded. The acousto-optical diffraction data as the laser probe is moved into the depth of the substrate are plotted against theoretical acousto-optic diffraction efficiency due to the decaying surface acoustic field into the substrate. The data are given by figures 26 to 29. The half diffraction efficiency point is about 18 acoustic wavelength into the substrate because the diffraction efficiency is proportional to the intensity of the acoustic field instead of the amplitude of the acoustic field. Very good agreement is found between the experimental results and the analytical results. The small discrepancy is believed due to the finite size of the probe beam and the error in setting the probe beam at zero-depth location, i.e. the surface. Figure 29 gives the measurement at 39 MHz as compared to all the other measurements at 26 MHz. Note that the acoustic field penetration becomes shallower at 39 MHz as compared to at 26 MHz.

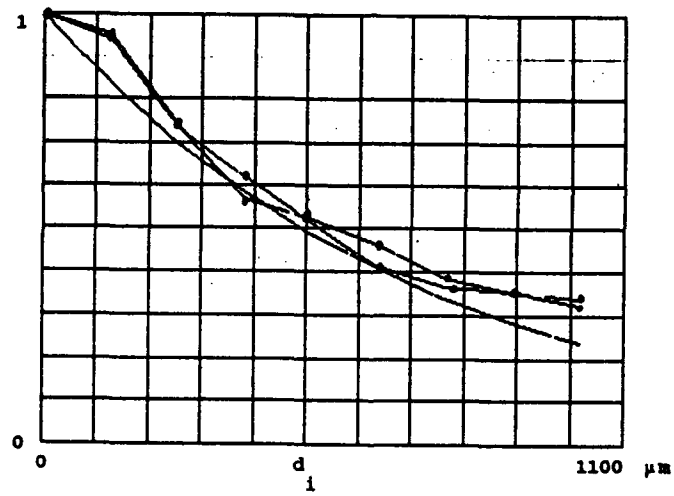

Figure 27, The relative diffraction efficiency of laser beam in the surface acoustic field of the crystal Teo2 as a function of the deepnees from the surface, vp=612.77 m/sec (theory), vp=613 m/sec (experiment) f=26 MHz, λ(laser)=0.6328 µm, P(laser)=3mW, distance between the tranducer and the measured point=14 mm

Acoustic attenuation measurements have been attempted. At 26 MHz, the measurement did not produce a noticeable number. Note that the attenuation for slow shear wave at 26 MHz is only 0.2 dB per cm. Measurements at higher frequencies were difficult due to the large amount of spurious shear waves in the crystal.

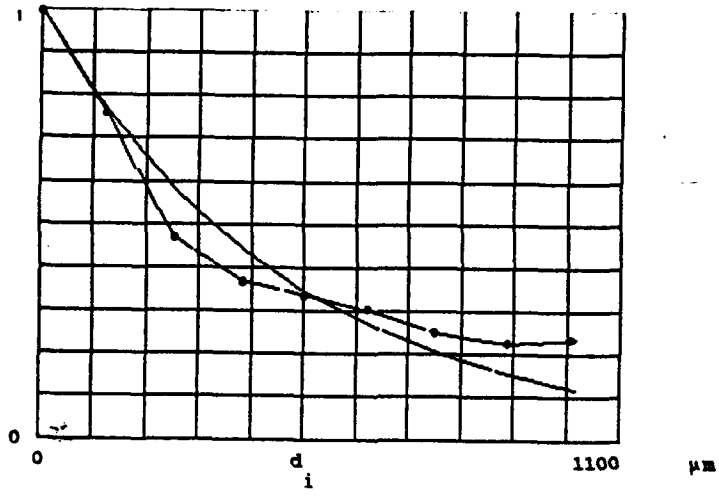

Figure 28,

The relative diffraction efficiency of laser beam in the surface acoustic field of the crystal Teo2 as a function of the deepnees from the surface, vp=612.77 m/sec (theory), vp=613 m/sec (experiment)
f=39 MHz, λ(laser)=0.6328 μm, P(laser)=3mW,
distance between the tranducer and the measured point=14
mm

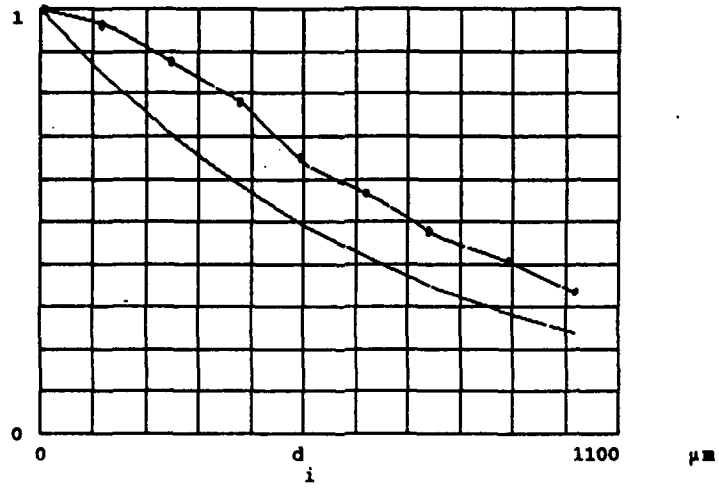

Figure 29,

The relative diffraction efficiency of laser beam in the surface acoustic field of the crystal Teo2 as a function of the deepnees from the surface, vp=612.77 m/sec (theory), vp=613 m/sec (experiment)
f=26 MHz, λ(laser)=0.6328 μm, P(laser)=3mW,
distance between the tranducer and the measured point=21 mm

2.4.5. EXPERIMENTAL RESULTS SUMMARY:

In summary, slow surface acoustic waves on the <110> direction of the (-110) surface of the TeO_2 crystal have been successfully launched by means of an edge bonded transducer. The existence of the surface acoustic wave is observed by optical schilearin method using an expanded HeNe laser beam. The field depth, the frequency dependence of the field depth, and the velocity of the surface acoustic wave have been probed by a focused HeNe laser beam. The experimental results are in excellent agreement with analytical results.

The existence and the physical properties of the slow surface acoustic wave on TeO_2 is verified. The slow velocity, the large field penetration depth, and the surface guiding feature of the slow surface acoustic wave shall be very useful in future high efficiency spatial light modulator and optical signal processing applications.

2.5. COMPARISON WITH BULK SLOW SHEAR WAVES:

A short term goal of a 70 microsecond 45 MHz bandwidth Bragg cell can be achieved with relative ease using bulk slow shear wave in TeO_2. Use of phase array technology may lower the acoustic power density for reduced nonlinearity and can be useful for eliminating degenerate frequency by producing frequency off-set in off-axis modes. The off-axis slow shear wave Bragg cell with long delay time requires an expansive and large crystal for dealing with the large Poynting vector walk-off angle. The large acoustic anisotropy in the slow shear bulk wave also requires use of large acoustic beam height, meaning large drive power requirement and large crystal size. Furthermore, the Fresnel diffraction of the acoustic waves within optical aperture must be removed by using diamond shaped transducer which sacrifices uniformity.

In comparison, the slow SAW have the following device advantages.

(1) Lower device cost due to smaller crystal size allowing batch fabrication.
(2) Saving of RF drive power by a factor of about 30 for 70μs device.
(3) Better optical output wavefront uniformity due to elimination of acoustic Fresnel diffraction within the optical aperture.
(4) Low spurious response in counter propagating Bragg cells due to high quality termination of the slow SAW by surface absorption.
(5) Improved temperature stability and device as well as system reliability due to less power dissipation.
(6) Ease in constructing beam steering phased array for further drive power reduction using surface overcoat layers.
(7) Potentially greater device bandwidth design by means of rotated substrate trading slow-SAW velocity for less acoustic attenuation.
(8) Reduced two-tone third order intermodulation product due to reduced power consumption and reduced acoustic attenuation across optical aperture.

The following table lists expected device performances for slow SAW and slow shear wave Bragg cell with 50 MHz bandwidth, 70 μs optical signal processing time at 633nm.

	Slow Shear Wave	Slow SAW
Crystal Size:	45mm x 9mm x 8mm	45mm x 3mm x 8mm
RF Power (50% eff.):	230 mW	8 mW
Cylindrical Lens:	Needed	Needed
Uniformity:	Fresnel Diffr.	Uniform.
Acoustic Termination:	Tough	Easier

3.0. POTENTIAL APPLICATIONS AND PHASE II RECOMMENDATIONS:

3.1. POTENTIAL APPLICATIONS:

From the previous discussion, it is noted that the major advantages of the slow SAW on (-110) cut TeO2 are drive power efficiency, lack of acoustic diffraction structure in the optical aperture and thus better uniformity, and easier for making more advanced devices such as counter propagating Bragg cells. The potential power efficiency of the device is very interesting since no acousto-optic modulators particularly large aperture devices has demonstrated power efficiency even close to this value. The extremely low power consumption and slow SAW velocity offer the potential of compact portable optical signal processing devices for versatile applications such as light vehicle or helicopter mounted transmitter locating, EW and ELINT systems for the Army. One particularly interesting application is for the construction of interferometric correlators using counter propagating slow SAW on TeO2. An trial design example is given below in comparison with a slow shear bulk wave design.

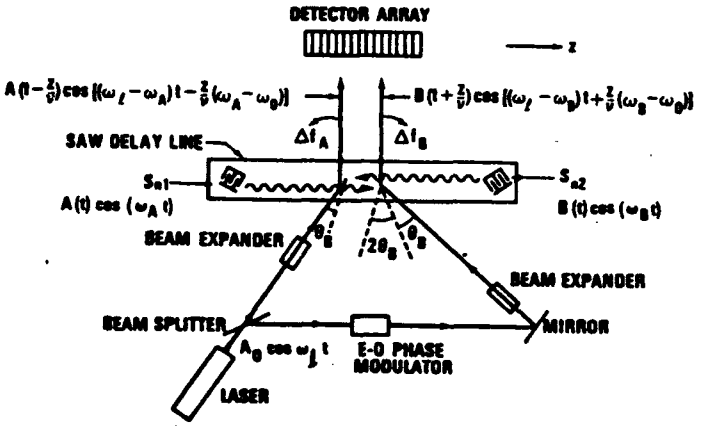

Figure 30, Counter Propagating Bragg Cell Correlator.

The device parameters are 20 to 70 μs signal processing time, up to 60 MHz bandwidth, two counter propagating acoustic beams diffracting two laser beams into one output. Optical signal processing devices of such long processing time can only use either the slow shear wave TeO_2 Bragg cell or the newly discovered slow SAW TeO_2 Bragg cell. First of all, a counter propagating beam acousto-optic design is needed for both approaches. Since the acoustic anisotropy in the (-110) plane for the two acoustic waves are nearly identical, the basic counter propagating configuration will be common to both cases.

3.1.1. TeO_2 COUNTER PROPAGATING AO BRAGG CELL:

Previous designs of counter propagating Bragg cell,[19] see figure 30, uses a nearly isotropic material, $LiNbO_3$. The (-110) plane of TeO_2 exhibits one of the highest known acoustic anisotropy making this design more difficult. A few design guidelines shall be discussed first before a design is attempted.

(1) For two signal correlation, the frequencies of the two acoustic waves is preferably equal to avoid beating. Difference frequency is allowed for four product correlators.
(2) The velocity of the two acoustic waves are preferably equal so that the two waveform envelopes will be of same scale.
(3) The cross interaction between each acoustic wave to the other laser beam shall be minimized.

With the following additional guide lines specifically for slow shear or slow SAW TeO_2 Bragg cells.

(4) For anisotropic Bragg diffraction, the two outputs from the two acousto-optical processes is preferably having same polarization, otherwise, an insertion loss will be incurred.
(5) Therefore, the optical output needs be on the <001> axis to allow identical acoustic velocity in the two acoustic beams.
(6) The degenerative on-axis tangential interaction shall be avoided.

Figure 31 illustrates the momentum diagram for one potential design. The two acoustic wave vectors need not necessarily be tangential to the ordinary index surface. However, the tangential case is one allowed solution if the acoustic frequency can be made high enough. Computer model originally programed for beam deflector design is employed to generate the numerical values for the incidence and exit angles in the anisotropic Bragg regime at various frequencies. Search is conducted to find the frequency such that the extraordinary ray is on the <001> direction by changing the acoustic vector off-axis angle, θ_a, (rotation about <-110>) and by rotating the Bragg interaction plane about the <110> axis, β. Note that at each acoustic off-axis angle, θ_a, there is only one acceptable value of β for a given acoustic frequency, f_o. Figure 32 gives the search results plotted as f_o versus β, and θ_a versus β. For a given Bragg plane

rotation, ß, figure 32 gives the corresponding value of tangential frequency with extraordinary ray on <001>, fo, and corresponding acoustic vector angle, θa.

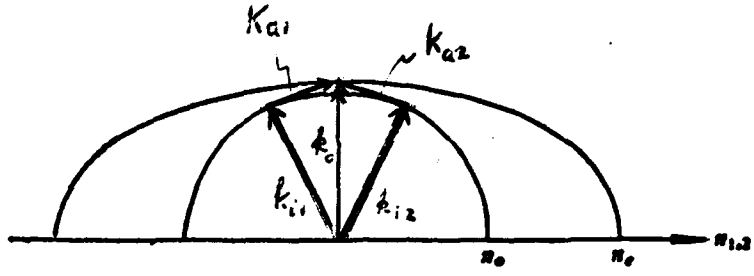

Figure 31, Momentum Diagram of an Anisotropic Counter Propagating Bragg Cell Design for Slow Shear or Slow SAW in TeO2.

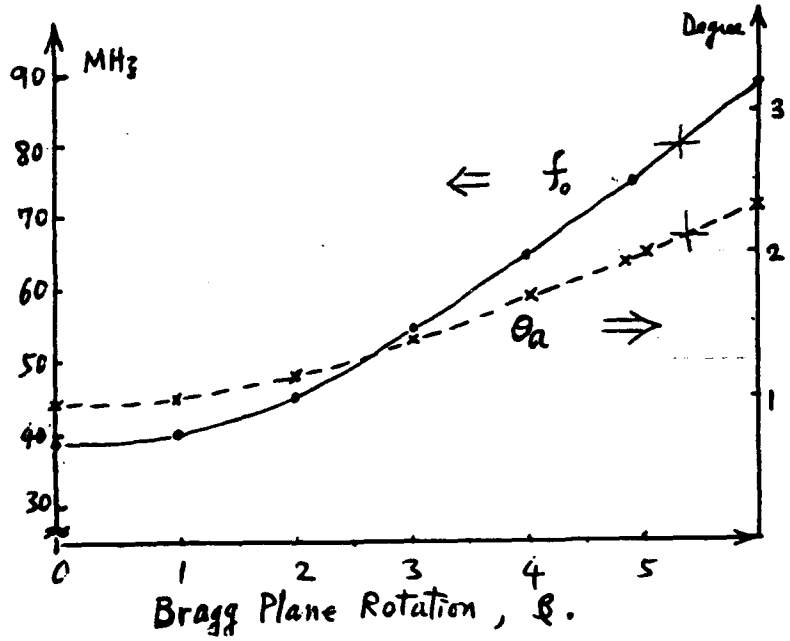

Figure 32, Acoustic Frequency for Extraordinary Ray to be on <001> Direction While Changing the Acoustic Off-Axis Angle, θa, and Rotating the Bragg Interaction Plane about <110> an Angle, ß.

From figure 32 it is noticed that in order to make extraordinary ray output on <001> at center frequency of 80 MHz for a 60 MHz bandwidth device, the Bragg plane rotation angle must be about 5.5 degree, and the acoustic vectors must be at ±2.15 degree off-axis. The two counter propagating acoustic vectors are thus separated by 4.3 degree which is more than enough to prevent optical cross-interaction. The crystal dimension for the counter propagating correlator is shown by figure 33. The acoustic wave velocity should be 0.6206 mm/μs, and the acoustic wave will walk-off at 21.5 degree from the transducer surface (phase vector). The two designs are given as follows for comparison.

Counter Propag. Designs	Slow Shear Design	Slow SAW Design
Bragg Plane Rotation:	5.5 degree	5.5 degree
Acoustic Off-Axis:	± 2.15 degree	± 2.15 degree
Acoustic Walk-Off:	± 21.5 degree	± 21.5 degree
Optical Inputs:	± 4.68 degree	± 4.68 degree
Optical Output:	0 degree	0 degree
Acoustic Center Freq.:	80 MHz	80 MHz
Bandwidth:	60 MHz	60 MHz
Optical Aperture:	50 μs/31 mm	50 μs/31 mm
Transducer Length:	0.6 mm	0.6 mm
Transducer Height:	**4.0 mm**	**0.22 mm**
Transducer Shape:	Diamond	Rectangle
RF Drive Power (50%):	500 mW	25.8 mW
Crystal Size:	40mm x 20mm x **9mm**	40mm x 20mm x **3mm**
Acoustic Termination:	Bouncing Off in Crystal	Absorpt on Surface

In these designs, the transducer length, L = 0.6 mm, is small relative to the slow shear wave beam deflectors because the input is ordinary ray and the output is extraordinary ray disqualifying the utilization of tangential phase matching gain. The main advantage of the slow SAW version design is low power consumption and smaller size. The low power dissipation on the device and the thinner substrate allows better temperature stability and thus less optical wavefront aberration and better reliability. Acoustic termination of slow shear wave devices has been a problem. Due to the high figure of merit and the large acoustic volume, the bouncing slow shear waves often produce lots of ghost diffractions. The ease in acoustic termination for the slow SAW device will also reduce the spurious response of the correlator.

It should be noted that in the counter propagation design, the ordinary ray optical input excludes the tangential acousto-optic gain. However, acoustic phased array[15,16] technology shall be applicable to provide enhanced acousto-optic interaction by beam steering. Due to the small acoustic wavelength for these slow waves, the phased array transducer elements will be very small making the high efficient non-planar arrays difficult to make. This problem can be resolved for the case of slow SAW devices. The SAW

velocity can be modulated by means of surface corrugation, etched pattern, or deposited surface overcoat. Such approaches no only are easier to make but also have at least 3 dB advantage over the planar phased array. In addition mode conversion ditches can be made with built-in delays. Use of these technologies on the slow SAW devices will further improve the slow SAW power efficiency, lower the power density and therefore the nonlinear acoustic spurious as well as intermodulation product. It will also pave ways for more sophisticated signal processing devices.

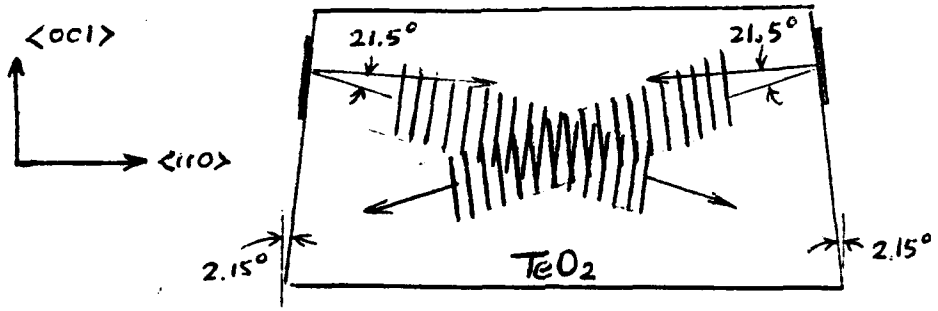

Figure 33, Crystal Dimension for the Counter Propagating Bragg Cell Correlator.

3.1.2. APPLICATIONS SUMMARY:

In summary, the extremely low power consumption of the slow SAW device is potentially useful for compact portable or avionics signal processing equipment applications. Low power consumption and lack of Fresnel diffraction in the optical aperture can contribute to better device performances due to less optical wavefront distortion from acoustic heating and uniform field. Ease of acoustic termination can also contribute to lower spurious responses. A design example is given for a counter propagating Bragg cell correlator design using the slow SAW and the slow shear wave in TeO2. The slow SAW design only require 25.8 mW of drive power, a factor of 20 better than the slow shear wave design.

In the examples given, the use of acoustic beam steering phased array is not yet considered. The bulk wave version can only employ the more primitive planar phased array due to fabrication difficulties. However, the slow SAW version can easily employ true phase array by modification of the SAW velocity through surface treatments. The result will be further reduction of drive power and power density requirements. Reduction

in acoustic nonlinearity byproducts such as two tone intermodulation products shall be expected. Thus, much cleaner spurious responses can be expected of the slow SAW acousto-optic devices in comparison to the bulk acousto-optic slow shear wave devices.

Many other new applications will be possible with the slow SAW. The long delay time and extremely low power consumption makes potential compact optical signal processors interesting for applications like emitter locating, radar processor, spread spectrum communication, and EW receivers. It can also contribute to efficient laser modulation and beam deflection devices particularly for IR sources which usually require very large RF drive power due to longer optical wavelength.

A potential branch off is newer technological opportunities. The slow shear TeO_2 acousto-optic device has enjoyed a unique position in long processing time optical processors. Although its useful bandwidth has been limited by acoustic attenuation to about 50 MHz, there is nothing else to replace it. The rotation of substrate about the <001> can adjust the slow SAW velocity form 613 m/s towards 840 m/s. It is expected that the acoustic attenuation will improve as the velocity increases. Thus, a trade-off between bandwidth and delay time in optical signal processing devices becomes available. Such capability has no counter part in bulk waves and can offer more useful bandwidth to communication and radar applications.

SAW technology has been very useful in transversal filter and other signal processing applications. The slow SAW can be tapped by 45 degree converters etched onto the substrate surface or by deposited piezoelectric thin film making very long time transversal signal processing possible.

3.2. PHASE II RECOMMENDATIONS:

The phase I program has discovered a very interesting slow surface acoustic wave in the <110> direction of the (-110) cut TeO_2 substrate. This slow SAW is unique in its slow velocity, deep field penetration, and pure particle displacement component. The velocity of surface acoustic waves are easily modulated by deposition of overcoat layers or surface corrugations. True delay phased array beam steering devices can be made with the slow SAW technology for improving Bragg cell efficiency and spurious responses. The slow SAW shall be very useful for making next generation optical signal processing devices. A phase II program is recommended for the development of demonstrative devices for optical signal processing especially for counter propagating Bragg cell correlators.

The proposed phase II program consists of six major tasks as follows.

(1) Optimize the transducer technology and the mode converter technology for the fabrication of slow SAW acousto-optic devices.

(2) Fabrication of high performance counter propagating slow SAW acousto-optic

Bragg cell using edge bonded transducers and total internal reflected laser beams for high quality compact correlators.

(3) Characterization of the counter propagating slow SAW Bragg cell.

(4) Experimental evaluation of the other slow SAW propagation directions by rotating the TeO_2 cut about the <001> axis, and determine their usefulness as acousto-optic signal processing devices.

(5) Development of true phase delay beam steering counter propagation Bragg cell based on the slow SAW on TeO_2, and demonstration of reduced intermodulation product.

(6) Reports and delivery.

A phase II proposal will be provided by the middle of February.

4.0 REFERENCES:

1, Cheng-Kuei Jen, et.al.,"Interactive Computer-Aided Analysis for Bulk Acoustic Waves in Materials of Arbitrary Anisotropy and Piezoelectricity," IEEE TRANS. Sonics and Ultrasonics, SU-32, No. 1, Jan. 1985.

2, C.K. Jen, et.al., "Interactive Computer-Aided Analysis of Bulk Waves Using A Personal Computer," 1984 Ultrasonics Symposium, Proceedings, p. 430.

3, E.L. Adler, et.al., "Interactive Computer-Aided Analysis of Surface Acoustic Waves Using A Personal Computer," Ultrasonics International 85, Proceedings.

4, A.J. Slobodnik, Jr., The Temperature Coeff. of Acoustic Surface Wave Velocity and Delay on Lithium Niobate, Lithium Tantalate, Quartz, and Tellurium Dioxide, 1972.

5, A.J. Slobodnik, Jr., E.D. Conway, and R.T. Delmonico, Microwave Acoustics Handbook, vol. 1A, Surface Wave Velocities, 1973.

6, T.L. Szabo and A.J. Slobodnik,Jr., Acoustic Surface Wave Diffraction and Beam Steering, 1973.

7, T. Shiosaki, "High-Speed Fabrication of High Quality Sputtered ZnO Thin Films for Bulk and Surface Wave Applications," 1978 IEEE Ultrasonics Symposium, p.100.

8, I.A. Viktorov, "Investigation of Methods for Exciting Rayleigh Waves," Soviet Phys-acoustics, vol 7, no. 3, p.236, 1962.

9, R.F. Humphryes, and E.A. Ash, "Acoustic Bulk-Surface-Wave Transducer," Electronic Lett., vol. 5, no. 9, p. 75, 1969. High efficiency (3.75 dB) bulk to surface acoustic wave conversion has been reported using saw-tooth shaped surface structure.

10, R. White, "Surface Elastic Waves," Proc. IEEE, Vol. 58, No. 8, p. 1238, 1970.

In this invited review paper, many surface acoustic wave excitation means has been described.

11, S.K. Yao, R.R. August, and D.B. Anderson, "Guided-Wave Acousto-Optic Interaction on Nonpiezoelectric Substrate," J. Appl. Phys., 49 (12), p.5728, 1978.

12, S.K. Yao, D. Weid, and R.M. Montgomery, "Guided Acoustic Traveling Wave Lens for High Speed Optical Scanners," Appl. Optics, 18, No. 4, p. 446, 1979.

13, S.K. Yao, "Acousto-Optic Interaction in a Planar Acoustic Waveguide," Appl. Optics, 17, No. 23, p.3837, 1978.

14, C.S. Tsai, L.T. Nguyen, and S.K. Yao, "A High Performance Acousto-Optic Guided Light Beam Device Using Intersecting Surface Acoustic Waves," Appl. Phy. Lett., 26, p. 140, 1975.

15, T.S. Chen and S.K. Yao,"A Novel Phased Array Acousto-Optic Bragg Cell," J. Appl. Phys., 60, p. 3732, 1986. This one talk about a new quasi-planar structure for a 1.3 GHz bandwidth GaP Bragg cell.

16, S.K. Yao,"Wideband Bragg Cell Efficiency Enhancement Techniques," SPIE Proc. 545, p. 72, 1985.

17, N.J. Berg, B.J. Udelson, and J.N. Lee, 1977 IEEE Ultrasonics Symposium, p.500, on use of surface acoustic waves on LiNbO3 substrate for acousto-optical interaction with focused laser beam reflecting off the surface from the substrate side. Many acousto-optical applications has been discussed.

18, N.J. Berg and J.N. Lee, An Enhanced Acousto-Optic Memory Correlator, 1978 IEEE Ultrasonics Symposium, p.95, Photorefractive property of LiNbO3 has been employed as optical memory and to correlate with acoustic signal.

19, I.J. Abramovitz, N.J. Berg and M.W. Casseday, "Interferometric Surface-Wave Acousto-Optic Time-Integrating Correlators," 1990 Ultrasonics Symposium, Proceedings, p. 483.